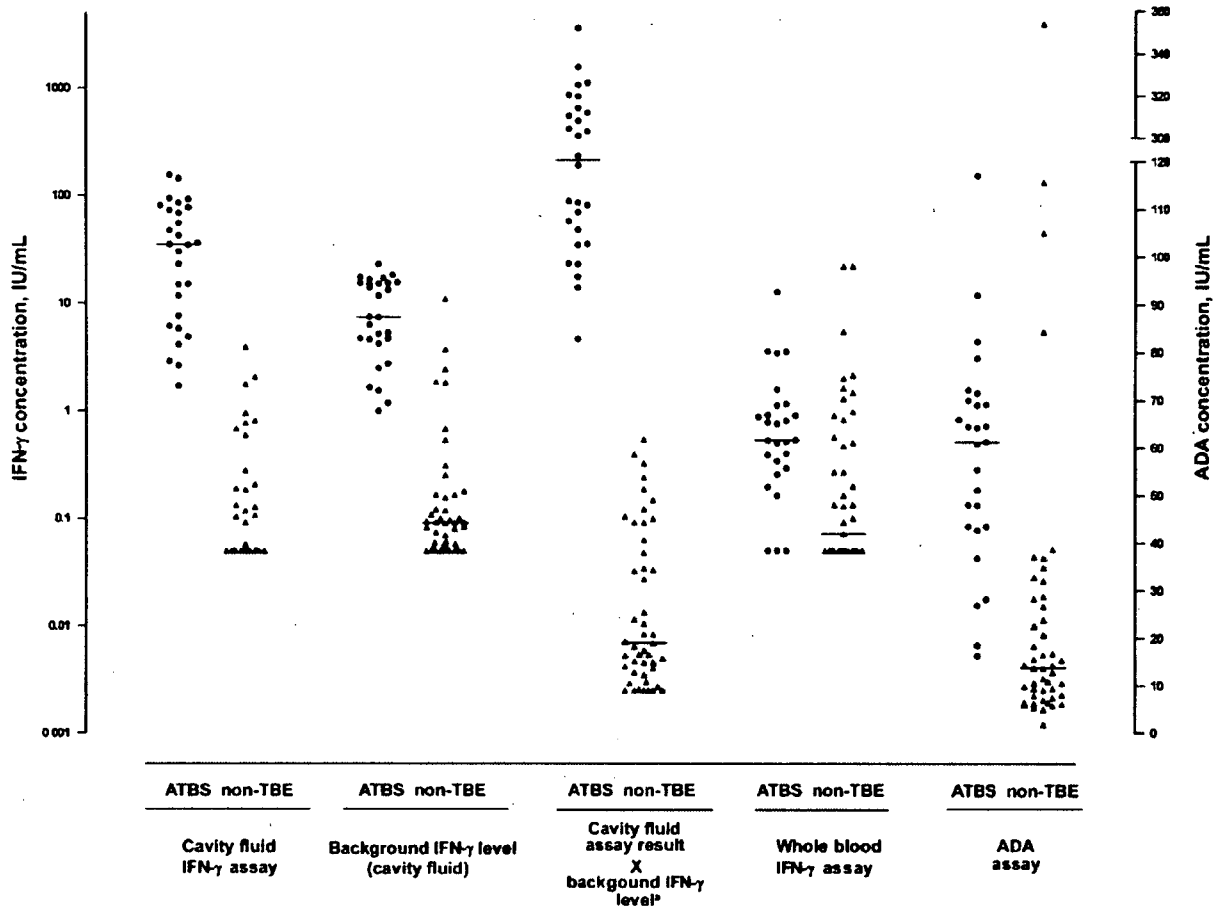

Figure 2. IFN-γ concentrations in cavity fluid and whole-blood and adenosine deaminase (ADA) concentrations in patients with active tuberculous serositis (ATBS) and in patients with nontuberculous effusion (non-TBE). Individual results of whole-blood IFN-γ, ADA, cavity fluid IFN-γ, and background control IFN-γ assays for patients with ATBS or non-TBE are shown. IFN-γ values are represented by the higher value of response to either early secretory antigenic target 6 (ESAT-6) or culture filtrate protein 10 (CFP-10) after subtraction of each background control IFN-γ value for the cavity fluid and whole-blood IFN-γ assays. Values for patients with ATBS and non-TBE are represented by closed circles and triangles, respectively. Horizontal lines in the columns represent the median value in each group. [a]Values calculated by multiplying the result of the cavity fluid IFN-γ assay by the background cavity fluid IFN-γ level and expressed as IU/mL^2.

for those with non-TBE. The median value of IFN-γ in the whole-blood IFN-γ assay was significantly higher for patients with ATBS than for patients with non-TBE, as was the median ADA value. For the whole-blood assay, none of the patients had indeterminate results, and 1 patient with ATBS was unavailable for testing. The ADA assay was not performed for 1 patient with tuberculosis.

Relative discriminative accuracy of the whole-blood, ADA, background IFN-γ, and cavity fluid assays was assessed in the area under the ROC curve (figure 3, table 3). The relative discriminative accuracy of the cavity fluid assay was statistically significantly different from that of the ADA ($P = .037$) and whole-blood assays ($P < .001$). The ROC curve for the cavity fluid assay was bowed further to the upper left, compared with that for the background IFN-γ level, but the areas under the ROC curve for the 2 assays were not statistically significantly different at the 5% level of type 1 error rate ($P = .74$).

Multivariate logistic regression was used as an aid in assessment of whether the cavity fluid assay added any diagnostic information to that yielded by the background IFN-γ level (table 4). Spearman's coefficient of correlation between the 2 measurements was 85%. The 2 measurements did not display statistical evidence of an interaction ($P = .84$). The Hosmer-Lemeshow test did not indicate a lack of fit ($P = .74$); thus, the predictors provide for a reasonably well calibrated model without data transformation. The cavity fluid assay displayed

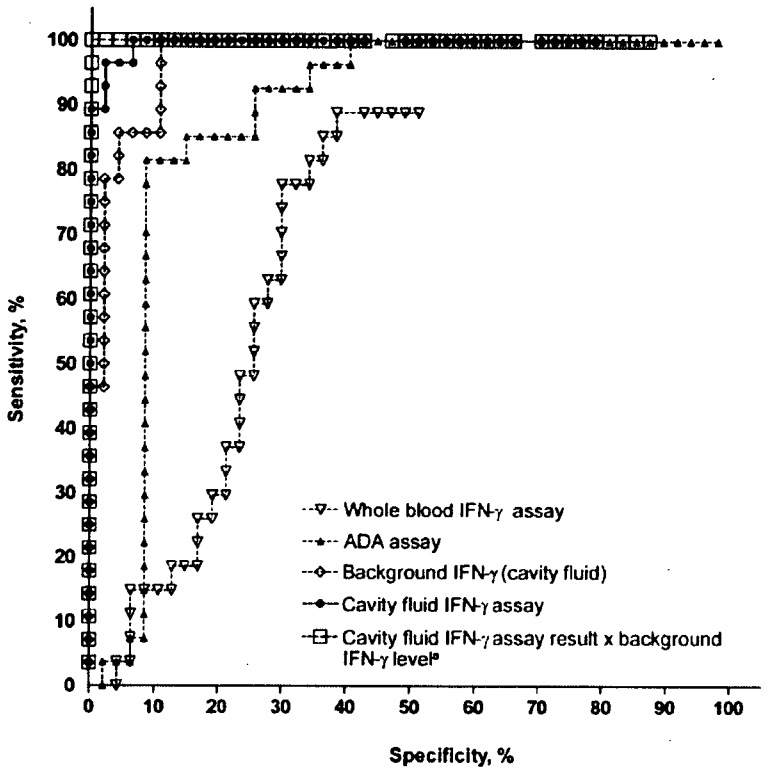

Figure 3. Receiver operating characteristic curves for 5 diagnostic methods used for patients with active tuberculous serositis and nontuberculous effusion. [a]Values calculated by multiplying the result of the cavity fluid IFN-γ assay by the background cavity fluid IFN-γ level and expressed as IU/mL[2].

a statistically significantly nonzero level of association with diagnostic status, even after adjustment for background IFN-γ concentrations, which supports the contention that the cavity fluid assay provides for improved diagnostic accuracy over that provided by the background IFN-γ level alone.

The cutoff value for each test was chosen to maximize specificity without significant loss of sensitivity. Table 5 shows sensitivity, specificity, likelihood ratio, and predictive value by cross classification. To calculate the predictive value, ~3.2% of pretest probability of ATBS in our specialist hospital for tuberculosis was used. As a result, both the likelihood ratio and predictive value of the cavity fluid assay were greater than those of the other assays. Furthermore, the value from when the results of the cavity fluid assay were multiplied by the background IFN-γ level was the most sensitive and specific predictor of ATBS.

DISCUSSION

Area under the ROC curve is the primary index for assessing the discriminative accuracy of a diagnostic method. Using this index, the cavity fluid assay displayed greater ability to discriminate ATBS than did either the ADA or whole-blood assays. The ROC curve index was not able to detect a difference in discriminative accuracy between unstimulated and specific antigen-stimulated IFN-γ response ex vivo. Nevertheless, a diagnostic advantage in assaying specific antigen-stimulated IFN-γ response was evident such that a multivariate logistic regression model provides a better fit to the clinical diagnosis when specific antigen-simulated IFN-γ production is included; the regression coefficient for the cavity fluid IFN-γ assay is statistically significantly different from zero. This better fit indicates improved calibration of the model. It is recognized that

Table 3. Comparison of diagnostic accuracy by area under the receiver operating characteristic (AUROC) curves.

Variable	AUROC curve (95% CI)	SE
Whole-blood IFN-γ assay	0.719 (0.598–0.838)	6.1
ADA assay	0.882 (0.799–0.965)	4.2
Background IFN-γ of cavity fluid	0.975 (0.946–1.004)	1.5
Cavity fluid IFN-γ assay[a]	0.996 (0.989–1.004)	0.4

[a] The value of the cavity fluid IFN-γ assay was defined as the difference between the determined higher IFN-γ value after stimulation with either early secretory antigenic target 6 or culture filtrate protein 10 and the background IFN-γ concentration.

Table 4. Multivariate logistic regression analysis.

Variable	Regression coefficient, log odds per IU/mL	SE	Likelihood ratio[a]	*P*	OR (95% CI)
Intercept	−3.47	0.79	...	...	...
Background IFN-γ of cavity fluid	0.34	0.23	3.10	.08	1.40 (0.80–2.19)
Cavity fluid IFN-γ assay	0.19	0.08	18.98	<.005	1.21 (1.03–1.42)

NOTE. Two explanatory variables were treated as continuous variables. Standardized ORs (each variable scaled to its interquartile range) were 5.6 for background IFN-γ and 55 for cavity fluid IFN-γ assay. Spearman's coefficient of correlation between the 2 measurements was 85%. The 2 measurements did not display statistical evidence of an interaction ($P = .84$). The Hosmer-Lemeshow test did not indicate a lack of fit ($P = .74$); thus, the predictors provide for a reasonably well calibrated model without data transformation.

[a] Likelihood ratio was determined using χ^2 test statistics and was single-degree-of-freedom.

area under the ROC curve is important but not always optimum in assessment of diagnostic tests, especially for predictive assessment of risk [21].

For the IFN-γ assay using cavity fluid, the IFN-γ concentration was significantly increased after antigen stimulation, compared with the background IFN-γ concentration, for every patient with ATBS (figure 1). It may be speculated that this result was because of further IFN-γ production by antigen-specific T cells in response to stimulation. We have obtained similar results for 30 patients with pleural effusion in whom active tuberculous pleuritis was strongly suspected clinically. Although, in these patients, definitive bacteriological evidence could not be obtained from pleural effusion specimens, antituberculous chemotherapy was effective (data not shown). In contrast, for the majority of 47 patients with effusion of nontuberculous etiology, IFN-γ concentrations did not increase after stimulation with antigens. This was also true for 5 of 47 patients with nontuberculous pleuritis who had relatively high background IFN-γ concentrations (>1 IU/mL).

In 3 of the patients with non-TBE who had a history of prior tuberculosis and in some of those without any clinical history of tuberculosis, IFN-γ concentrations were slightly increased in cavity fluid after stimulation, compared with background IFN-γ concentrations. Similarly, results of the whole-blood assay were positive for all of these patients. It may be speculated that when patients with a history of tuberculosis encounter serositis attributable to causes other than tuberculosis, preexisting antigen-specific memory T cells in peripheral blood also appear in the effusion and produce IFN-γ through stimulation by antigens in vitro. If diagnostic evaluation was made only on the basis of measuring an antigen-specific IFN-γ response or on a count of IFN-γ–producing cells by enzyme-linked immunospot assay [22], there is a possibility that some patients with an effusion of nontuberculous etiology who have incidental latent tuberculosis infection (LTBI) will receive a false-positive diagnosis. In such cases, non-TBE with LTBI can be differentially diagnosed from ATBS on the basis of low background IFN-γ concentration (figure 1). We speculate that high background IFN-γ concentrations in patients with ATBS are a reflection of the ongoing active status of the local type I helper T cellular immune response. High IFN-γ concentrations in the supernatant of pleural effusion specimens from patients with tuberculous pleuritis have been reported [3, 7, 23, 24]. However, it has also been demonstrated that the IFN-γ concentration can be high in those patients with an effusion of nontuberculous etiology [7]. In our study, 5 of 47 patients with non-TBE (i.e., *M. avium* pleuritis, cancerous pleuritis, and parapneumonia) had background IFN-γ concentrations that were similar to those found in patients with ATBS (>1 IU/mL). Thus, it appears that specificity of the background IFN-γ level may be limited and that false-positive responses can occur. The cavity fluid assay can assess both background IFN-γ and antigen-specific IFN-γ responses simultaneously, and it is possible to compensate for the fault mutually by assessing the value of both responses together. We demonstrated that the values from when the result of the cavity fluid assay was multiplied by the result of the background IFN-γ possibly could be used to accurately diagnose active tuberculous effusion (figure 2, table 5).

Although both the enzyme-linked immunospot assay using the peripheral blood and whole-blood IFN-γ assay have been reported for the diagnosis of tuberculosis, the results of these assays were also positive for people with LTBI. The whole-blood assay also has been reported to be highly specific for *M. tuberculosis* infection, but it cannot discriminate between active tuberculosis and LTBI. In our study, the group of patients who did not have ATBS likely contained a number of subjects with LTBI. Indeed, 3 patients with non-TBE who had a documented history of prior tuberculosis had positive whole-blood assay results. Similarly, 11 other patients who did not have ATBS had positive whole-blood assay results but had no clear history of tuberculosis or evidence of an old tuberculous lesion on chest radiograph (table 5). Because of the high specificity (>98%) of the whole-blood IFN-γ assay among a young population with no risk for tuberculosis [19], we speculated that these patients were latently infected with tuberculosis, reflecting their age and an era when tuberculosis was prevalent in Japan. An additional

Table 5. Comparison of diagnostic accuracy of adenosine deaminase (ADA), whole-blood, and cavity fluid IFN-γ assays.

Variable	Cutoff value	Result, positive: negative		Sensitivity, % (95% CI)	Specificity, % (95% CI)	Positive likelihood ratio	Negative likelihood ratio	PPV[a]	NPV[a]
		ATBS group	Non-TBE group						
Whole-blood IFN-γ assay	0.281	21:6	14:33	77.8 (57.7–91.4)	70.2 (55.1–82.7)	2.6	3.2	7.94	99.0
ADA assay	40.700	22:5	4:43	81.5 (61.9–93.7)	91.5 (79.6–97.6)	9.6	4.9	24.5	99.3
Background IFN-γ of cavity fluid	2.456	24:4	2:45	85.7 (67.3–96.0)	95.6 (85.5–99.5)	20.1	6.7	39.7	99.5
Cavity fluid IFN-γ assay[b]	2.352	27:1	1:46	96.4 (81.7–99.9)	97.8 (88.7–99.95)	45.3	27.4	60.3	99.9
Cavity fluid assay result times the background IFN-γ level[c]	2.590	28:0	0:47	100 (87.7–100)	100 (92.5–100)	...	...	100.0	100.0

NOTE. For the whole-blood assay, none of the patients had indeterminate results, and 1 patient with active tuberculous serositis (ATBS) was unavailable. The ADA assay was not performed for 1 patient with ATBS. Non-TBE, nontuberculous effusion; NPV, negative predictive value; PPV, positive predictive value.

[a] Pretest probability of active tuberculous effusion in our department of respiratory medicine was 3.2%

[b] The result of the cavity fluid IFN-γ assay was defined as the difference between the determined higher value of IFN-γ after stimulation with either early secretory antigenic target 6 or culture filtrate protein 10 and the background IFN-γ concentration.

[c] The values from when the result of the cavity fluid IFN-γ assay was multiplied by the background IFN-γ level.

finding was that the whole-blood assay result was negative for 6 of 27 patients with ATBS. In this study, results of the whole-blood assay showed reduced sensitivity (77.8%), compared with the sensitivity found in previous reports (89%) [19]. It has been reported that T cells that are specific for tuberculous antigens are sequestered from the circulation to the pleural cavity in patients with pleural tuberculosis [22]. The migration of antigen-specific T cells from peripheral blood to the active site of disease was thought to be 1 possible cause of lower than previously reported sensitivity of the whole-blood assay.

ADA in the supernatant of pleural effusion is reported as a diagnostic marker for tuberculous pleuritis [25–27]. The sensitivity and specificity of the ADA assay were reported to be 47.1%–100% and 0%–100%, respectively [28]. In our study, ADA concentrations were significantly higher in patients with ATBS than in patients with non-TBE. With regard to both sensitivity and specificity, the ADA assay had better performance than did the whole-blood assay for diagnosis of ATBS (table 5). However, in 4 of 47 patients with non-TBE (attributable to asbestosis, adenocarcinoma, and parapeumonic pleural effusion), ADA concentrations were as high as those in patients with ATBS. Furthermore, in some patients with active pleural and peritoneal tuberculosis, the ADA concentration was as low as that in patients with non-TBE. These false-positive and false-negative cases will be problematic when physicians make decisions regarding the initiation of long-term antituberculous chemotherapy.

In conclusion, we reported a highly sensitive and specific diagnostic method for active tuberculous pleuritis, tuberculous peritonitis, and pericarditis in which IFN-γ responses were measured after stimulation of cavity fluid cells with *M. tuberculosis*–specific antigens. The cavity fluid IFN-γ assay could be a noninvasive method for accurately and promptly diagnosing tuberculous serositis in patients in whom active tuberculosis in the cavity space is clinically suspected but for which no bacteriological evidence can be obtained.

Acknowledgments

We thank Yurika Ito, Ayako Watanabe, and Yasuko Inoue, for their technical assistance with the laboratory assays, and Drs. Kazuhiro Uchiyama, Toshiki Tamura, and Hajime Goto, for their support.

Financial support. The Ministry of Health, Labor and Welfare of Japan.

Potential conflicts of interest. All authors: no conflicts.

References

1. Dye C. Global epidemiology of tuberculosis. Lancet 2006; 367:938–40.
2. Gopi A, Madhavan SM, Sharma SK, Sahn SA. Diagnosis and treatment of tuberculous pleural effusion in 2006. Chest 2007; 131:880–9.
3. Ribera E, Ocana I, Martinez-Vazquez JM, Rossell M, Espanol T, Ruibal A. High level of interferon gamma in tuberculous pleural effusion. Chest 1988; 93:308–11.
4. Ocana I, Martinez-Vazquez JM, Segura RM, Fernandez-De-Sevilla T, Capdevila JA. Adenosine deaminase in pleural fluids: test for diagnosis of tuberculous pleural effusion. Chest 1983; 84:51–3.
5. Greco S, Girardi E, Masciangelo R, Capoccetta GB, Saltini C. Adenosine deaminase and interferon gamma measurements for the diagnosis of tuberculous pleurisy: a meta-analysis. Int J Tuberc Lung Dis 2003; 7: 777–86.
6. Riantawan P, Chaowalit P, Wongsangiem M, Rojanaraweewong P. Diagnostic value of pleural fluid adenosine deaminase in tuberculous pleuritis with reference to HIV coinfection and a Bayesian analysis. Chest 1999; 116:97–103.
7. Villena V, Lopez-Encuentra A, Echave-Sustaeta J, Martin-Escribano P, Ortuno-de-Solo B, Estenoz-Alfaro J. Interferon-gamma in 388 immunocompromised and immunocompetent patients for diagnosing pleural tuberculosis. Eur Respir J 1996; 9:2635–9.
8. Burgess LJ, Maritz FJ, Le Roux I, Taljaard JJ. Combined use of pleural adenosine deaminase with lymphocyte/neutrophil ratio: increased specificity for the diagnosis of tuberculous pleuritis. Chest 1996; 109:414–9.
9. Ocana I, Ribera E, Martinez-Vazquez JM, et al. Adenosine deaminase activity in rheumatoid pleural effusion. Ann Rheum Dis 1988; 47: 394–7.
10. Laniado-Laborin R. Adenosine deaminase in the diagnosis of tuberculous pleural effusion: is it really an ideal test? A word of caution. Chest 2005; 127:417–8.

11. Gupta UA, Chhabra SK. Diagnosing tubercular pleural effusions. Chest 2005; 127:1078; author reply 1078–9.
12. Barnes PF, Mistry SD, Cooper CL, Pirmez C, Rea TH, Modlin RL. Compartmentalization of a $CD4^+$ T lymphocyte subpopulation in tuberculous pleuritis. J Immunol 1989; 142:1114–9.
13. Stead WW, Eichenholz A, Stauss HK. Operative and pathologic findings in twenty-four patients with syndrome of idiopathic pleurisy with effusion, presumably tuberculous. Am Rev Tuberc 1955; 71:473–502.
14. Andersen P, Munk ME, Pollock JM, Doherty TM. Specific immune-based diagnosis of tuberculosis. Lancet 2000; 356:1099–104.
15. van Pinxteren LA, Ravn P, Agger EM, Pollock J, Andersen P. Diagnosis of tuberculosis based on the two specific antigens ESAT-6 and CFP10. Clin Diagn Lab Immunol 2000; 7:155–60.
16. Arend SM, Andersen P, van Meijgaarden KE, et al. Detection of active tuberculosis infection by T cell responses to early-secreted antigenic target 6-kDa protein and culture filtrate protein 10. J Infect Dis 2000; 181:1850–4.
17. Munk ME, Arend SM, Brock I, Ottenhoff TH, Andersen P. Use of ESAT-6 and CFP-10 antigens for diagnosis of extrapulmonary tuberculosis. J Infect Dis 2001; 183:175–6.
18. Arend SM, Engelhard AC, Groot G, et al. Tuberculin skin testing compared with T-cell responses to *Mycobacterium tuberculosis*–specific and nonspecific antigens for detection of latent infection in persons with recent tuberculosis contact. Clin Diagn Lab Immunol 2001; 8:1089–96.
19. Mori T, Sakatani M, Yamagishi F, et al. Specific detection of tuberculosis infection: an interferon-gamma–based assay using new antigens. Am J Respir Crit Care Med 2004; 170:59–64.
20. DeLong ER, DeLong DM, Clarke-Pearson DL. Comparing the areas under two or more correlated receiver operating characteristic curves: a nonparametric approach. Biometrics 1988; 44:837–45.
21. Cook NR. Use and misuse of the receiver operating characteristic curve in risk prediction. Circulation 2007; 115:928–35.
22. Wilkinson KA, Wilkinson RJ, Pathan A, et al. Ex vivo characterization of early secretory antigenic target 6-specific T cells at sites of active disease in pleural tuberculosis. Clin Infect Dis 2005; 40:184–7.
23. Villena V, Lopez-Encuentra A, Pozo F, et al. Interferon gamma levels in pleural fluid for the diagnosis of tuberculosis. Am J Med 2003; 115: 365–70.
24. Barnes PF, Fong SJ, Brennan PJ, Twomey PE, Mazumder A, Modlin RL. Local production of tumor necrosis factor and IFN-gamma in tuberculous pleuritis. J Immunol 1990; 145:149–54.
25. Banales JL, Pineda PR, Fitzgerald JM, Rubio H, Selman M, Salazar-Lezama M. Adenosine deaminase in the diagnosis of tuberculous pleural effusions: a report of 218 patients and review of the literature. Chest 1991; 99:355–7.
26. Burgess LJ, Maritz FJ, Le Roux I, Taljaard JJ. Use of adenosine deaminase as a diagnostic tool for tuberculous pleurisy. Thorax 1995; 50:672–4.
27. Valdes L, San Jose E, Alvarez D, Valle JM. Adenosine deaminase (ADA) isoenzyme analysis in pleural effusions: diagnostic role, and relevance to the origin of increased ADA in tuberculous pleurisy. Eur Respir J 1996; 9:747–51.
28. Goto M, Noguchi Y, Koyama H, Hira K, Shimbo T, Fukui T. Diagnostic value of adenosine deaminase in tuberculous pleural effusion: a meta-analysis. Ann Clin Biochem 2003; 40:374–81.

LETTERS

Dominant-negative mutations in the DNA-binding domain of STAT3 cause hyper-IgE syndrome

Yoshiyuki Minegishi[1], Masako Saito[1], Shigeru Tsuchiya[2], Ikuya Tsuge[3], Hidetoshi Takada[4], Toshiro Hara[4], Nobuaki Kawamura[5], Tadashi Ariga[5], Srdjan Pasic[6], Oliver Stojkovic[7], Ayse Metin[8] & Hajime Karasuyama[1]

Hyper-immunoglobulin E syndrome (HIES) is a compound primary immunodeficiency characterized by a highly elevated serum IgE, recurrent staphylococcal skin abscesses and cyst-forming pneumonia, with disproportionately milder inflammatory responses, referred to as cold abscesses, and skeletal abnormalities[1]. Although some cases of familial HIES with autosomal dominant or recessive inheritance have been reported, most cases of HIES are sporadic, and their pathogenesis has remained mysterious for a long time. Here we show that dominant-negative mutations in the human signal transducer and activator of transcription 3 (*STAT3*) gene result in the classical multisystem HIES. We found that eight out of fifteen unrelated non-familial HIES patients had heterozygous *STAT3* mutations, but their parents and siblings did not have the mutant *STAT3* alleles, suggesting that these were *de novo* mutations. Five different mutations were found, all of which were located in the STAT3 DNA-binding domain. The patients' peripheral blood cells showed defective responses to cytokines, including interleukin (IL)-6 and IL-10, and the DNA-binding ability of STAT3 in these cells was greatly diminished. All five mutants were non-functional by themselves and showed dominant-negative effects when co-expressed with wild-type *STAT3*. These results highlight the multiple roles played by STAT3 in humans, and underline the critical involvement of multiple cytokine pathways in the pathogenesis of HIES.

Elevated serum IgE is a hallmark of many allergic disorders[2]. Curiously enough, the hyper-IgE state is also observed in some primary immunodeficiency disorders, such as HIES, Wiskott-Aldrich syndrome, Omenn syndrome and Comèl-Netherton syndrome[3]. HIES (OMIM number 243700) was first reported in 1966 as Job's syndrome (OMIM number 147060)[4,5], but its underlying cause is still unknown, unlike the other three syndromes. In most cases of HIES, the clinical manifestations extend over multiple systems in the body, including the immune system, skeletal/dental system and soft tissue[6]. In contrast, the abnormalities in familial autosomal recessive (AR)-HIES patients seem to be confined to the immune system[7]. We previously identified a homozygous mutation of the tyrosine kinase 2 (*TYK2*) gene in a patient who showed AR-HIES and susceptibility to intracellular bacterial infections[8]. TYK2 is a non-receptor tyrosine kinase belonging to the JAK family[9,10]. The patient's cells expressed no detectable TYK2 protein and displayed defects in multiple cytokine signals, including the signalling pathways for IL-6, IL-10, IL-12, IL-23 and type I IFN. The cytokine signals were successfully restored by introducing the intact *TYK2* gene into the patient's cells. These multiple defects probably account for the patient's complex clinical manifestations[8]. The identification of a TYK2 deficiency in this HIES patient indicated to us that, besides TYK2, one or more molecules shared by multiple cytokine signalling pathways might also cause HIES.

To explore this possibility, we first examined the responses to IL-6, IL-10, IL-12 and IFNα of peripheral blood cells from two patients (patient 1 and patient 2) who showed characteristics of multisystem HIES, including skeletal/dental abnormalities, skin abscesses, cyst-forming pneumonia and highly elevated serum IgE (Supplementary Table 1). The patients' B cells secreted IgM normally when stimulated with Epstein–Barr virus (EBV) infection (Fig. 1a). However, additional stimulation with IL-6 induced no significant increase in IgM secretion in the patients' B cells, unlike in the control B cells (Fig. 1a). Moreover, the suppression of lipopolysaccharide-induced production of TNFα by IL-10 deteriorated in the patients' macrophages (Fig. 1b). Thus, both the IL-6 and IL-10 pathways were defective in these HIES patients, as in the TYK2-deficient patient (Fig. 1a and 1b). In contrast, neither IL-12 nor IFNα signalling was impaired in the HIES patients, unlike in the TYK2-deficient patient (Fig. 1c and 1d). The HIES patients' T cells produced IFNγ normally in response to IL-12 (Fig. 1c), and their peripheral blood mononuclear cells (PBMCs) showed normal upregulation of transcripts for two IFN-inducible genes, *NMI* and *MX1* (also known as *MxA*), in response to IFNα (Fig. 1d). These observations indicated a possible abnormality in one or more molecules that was shared by the IL-6 and IL-10 signals but not essential for the IL-12 and IFNα pathways.

An array of cytokine signals is transduced by different combinations of JAK family kinases and STATs[9,10]. When cytokines bind to their receptors, receptor-associated JAKs are activated to phosphorylate STATs, which in turn dimerize and translocate to the nucleus, where they activate target genes. In a survey of possible abnormalities in this signal cascade, we identified heterozygous mutations in the STAT3 DNA-binding domain in both patients: a single amino acid deletion (ΔV463) in patient 1 and a mis-sense mutation (R382W) in patient 2 (Fig. 2). Because STAT3 is shown to be activated in response to a wide variety of cytokines, growth factors, and hormones[11,12], we thought that its mutation could well account for the patients' complex clinical manifestations extending over multiple systems. Further analysis of the STAT3 complementary DNA sequences in thirteen more unrelated patients with non-familial HIES identified heterozygous mutations in six of these patients (patients 3–8; see Supplementary Table 1 for clinical summary), and all of these mutations were located in the DNA-binding domain of STAT3: ΔV463 in patient 3 and patient 8, like in patient 1; R382Q in patient 4; H437Y in patient 5; T389I in patient 6; R382W in patient 7, like in patient 2 (Fig. 2). The five different STAT3 mutations found in the

[1]Department of Immune Regulation, Tokyo Medical and Dental University Graduate School, Tokyo 113-8519, Japan. [2]Department of Pediatrics, Tohoku University Graduate School of Medicine, Sendai 980-8575, Japan. [3]Department of Pediatrics, Fujita Health University, Aichi 470-1192, Japan. [4]Department of Pediatrics, Kyushu University, Fukuoka 812-8582, Japan. [5]Department of Pediatrics, Hokkaido University Graduate School of Medicine, Sapporo 060-8638, Japan. [6]Pediatric Immunology, Mother and Child Health Institute, Belgrade 110 70, Serbia. [7]Laboratory for Forensic Genetics, Institute of Forensic Medicine, University of Belgrade, Belgrade 110 70, Serbia. [8]Pediatric Immunology Department, SB Ankara Diskapi Children's Hospital, Ankara 06110, Turkey.

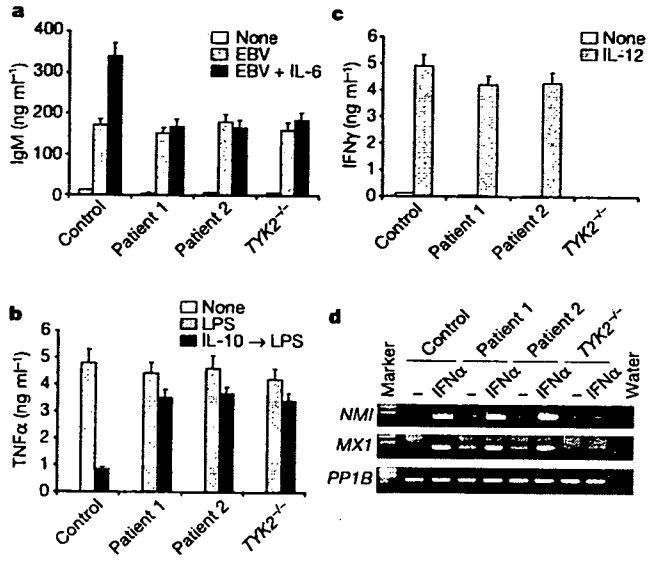

Figure 1 | Impaired responses to IL-6 and IL-10 in HIES patients' cells. **a**, IgM levels in culture medium of PBMCs from a control subject, two HIES patients (patient 1 and patient 2), and the TYK2-deficient patient, cultured for 7 days without stimulation, with EBV alone or with EBV and IL-6. **b**, TNFα levels in culture medium of macrophages from the same subjects, cultured without or with lipopolysaccharide (LPS) stimulation for 48 h, or with IL-10 treatment for 24 h before lipopolysaccharide stimulation. **c**, IFNγ in culture medium of $CD4^+$ T cells from the same subjects, cultured for 24 h without or with IL-12. Error bars show standard deviations (**a**–**c**). **d**, *NMI*, *MX1* and cyclophilin B (*PPIB*) transcript levels in PBMCs from the same subjects were unstimulated or stimulated with IFNα for 2 h.

eight patients were all confirmed by sequencing their genomic DNA, and no sequence alterations were detected in any other parts of *STAT3*, *TYK2* or *JAK1*. The DNA-binding domain of STAT3 is highly conserved among different species in its amino acid sequence, and the alterations identified in the patients' *STAT3* gene were statistically highly significant in population genetics ($P < 10^{-15}$, Fisher's exact probability test), as judged by the fact that such alterations were not found in 1,000 unrelated healthy individuals analysed, including at least 100 controls from the patients' ethnic group. *STAT3* is located on human chromosome 17q21, but not 4q, which was reported to contain a disease locus for familial AD-HIES[13]. None of the eight HIES patients in the present study had a known family history of HIES, and no mutation was detected in the *STAT3* cDNAs from all the parents and seven siblings of the patients, even though an analysis of multiple polymorphic markers confirmed the biological parent–child relationship (data not shown). Therefore, the mutations are likely to have occurred *de novo* in the HIES patients.

We next evaluated the biological significance of the STAT3 mutations. The STAT3 protein levels were comparable in all the EBV-transformed B-cell lines established from patients 1–6 and a control subject, and the extent of the tyrosine phosphorylation on STAT3 induced by IFNα stimulation was also comparable (Fig. 3a). Furthermore, all the mutant proteins formed a complex with wild-type STAT3 as efficiently as did wild-type STAT3, as judged by the co-immunoprecipitation of wild-type and mutant STAT3 proteins co-expressed in COS7 cells (Fig. 3b). However, nuclear extracts isolated from the patients' cells stimulated with IFNα contained much lower amounts of active STAT3 that could bind to target DNA compared with nuclear extracts from the control cells, whereas the DNA-binding activity of STAT1 was intact in the patients' cells (Fig. 3c). This finding was consistent with a previous report showing that changing codons 461 to 463 in STAT3 from Val-Val-Val to Ala-Ala-Ala resulted in the impairment of STAT3's DNA-binding activity[14]. Thus, the genetic mutations identified in the HIES patients seemed to result in the impairment of the DNA-binding activity of STAT3 and most likely that of heterodimers between mutant and wild-type STAT3 molecules. A similar impairment of DNA-binding activity in STAT1 protein was recently reported in cells isolated from patients carrying a heterozygous mutation in the DNA-binding domain of STAT1 (ref. 15).

When wild-type STAT3 was exogenously expressed—together with a luciferase reporter gene containing STAT3-responsive elements—in human HeLa cells in which the endogenous STAT3 was knocked down, fivefold upregulation of luciferase activity in response to IFNα was detected (Fig. 4a). In contrast, none of the STAT3 mutants conferred any significant increase of luciferase activity on the HeLa cells in response to IFNα, demonstrating a loss of function of the STAT3 mutants. To explore the possibility that the STAT3 mutant proteins function as dominant-negative, wild-type STAT3 or the individual mutants were exogenously expressed in IL-6-responsive HepG2 cells and IL-10-responsive MC/9 cells (Fig.

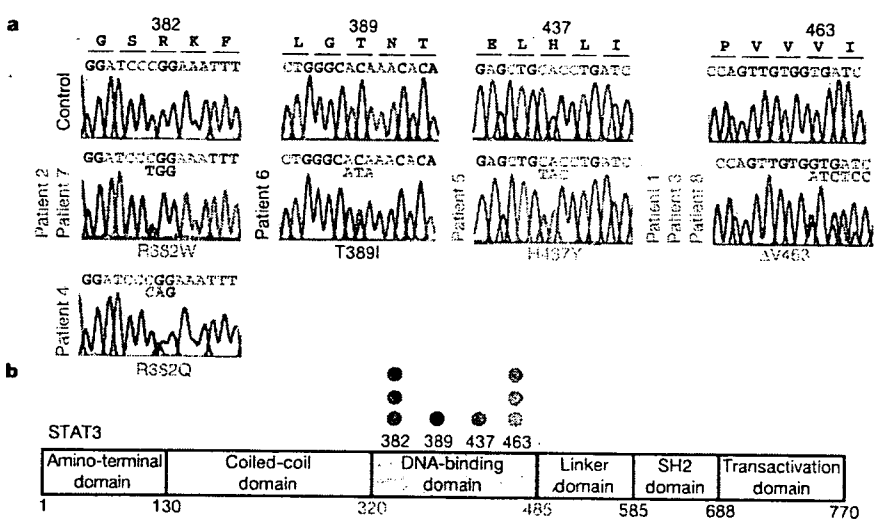

Figure 2 | Heterozygous mutations in the DNA-binding domain of STAT3 from eight HIES patients. **a**, Electropherograms showing partial *STAT3* cDNA sequences from a control subject and the eight HIES patients. **b**, The structure of STAT3 is shown schematically, and the positions of the mutations identified in the eight patients are indicated.

4b and 4c). In HepG2 cells transfected with empty vector together with the reporter luciferase gene, the luciferase activity was upregulated as much as 3.5 times its basal level in response to IL-6 stimulation. The IL-6-induced upregulation of luciferase activity was augmented in HepG2 cells transfected with wild-type *STAT3* by up to 5.5 times, whereas it was severely impaired in cells transfected with any of the mutant *STAT3*s, showing at most a 2-fold increase (Fig. 4b). Moreover, the IL-10-induced downregulation of surface KIT (C-Kit) expression was severely impaired in MC/9 cells transfected with any of the mutant STAT3s, unlike those with empty vector or wild-type *STAT3* (Fig. 4c). Thus, all the STAT3 mutants identified in the HIES patients displayed dominant-negative effects when co-expressed with wild-type STAT3.

The DNA-binding activity of STAT3 in the IFNα-stimulated patients' cells was not totally abrogated, although it was only approximately one-fourth that of control cells (Fig. 3b). This residual STAT3 activity might have rescued the patients from early embryonic death, which is observed in STAT3-deficient mice[16]. In contrast, its diminished activity might have an impact on the development and functions of multiple organ systems, leading to compound clinical manifestations of HIES, given STAT3's role in the signalling pathways of a variety of soluble factors, including the IL-6-family cytokines (IL-6, IL-11, IL-27, IL-31, LIF, OSM, CNTF and cardiotrophin-1), the IFN-family cytokines (IL-10, IL-19, IL-20, IL-22, IL-24, IL-26, IFNα/β and IFNγ), the IL-2-family cytokines (IL-2, IL-7, IL-9, IL-15 and IL-21), IL-5, IL-23, CSF3/G-CSF, EGF, CSF1 and leptin[12,17,18].

It has been shown that STAT3 has important roles in the differentiation of both osteoblasts and osteoclasts *in vitro*[19], and mice deficient for STAT3 in osteoblasts show an osteoporotic phenotype[20]. When osteoclasts were generated from peripheral blood monocytes in culture with CSF1/M-CSF and TNFSF11/RANKL, those from the HIES patients with the STAT3 mutations showed higher bone-resorption activity compared to those from control subjects (Supplementary Fig. 1). This may reflect the skeletal/dental abnormalities

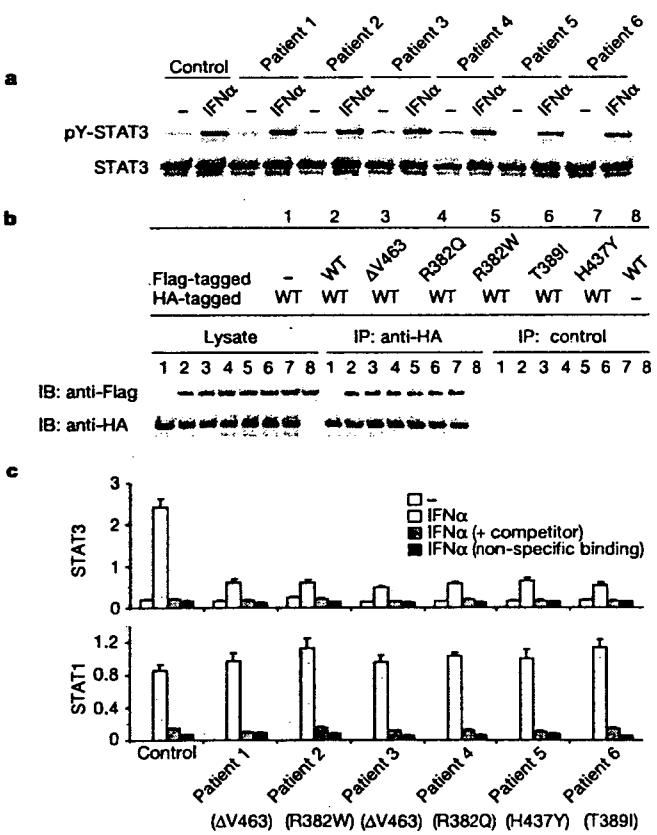

Figure 3 | Diminished DNA-binding activity of STAT3 in the HIES patients' cells. **a**, Total and tyrosine-phosphorylated (pY-) STAT3 proteins detected by immunoblotting. EBV-transformed B-cell lines (EBV-LCL) established from a control subject and the HIES patients were unstimulated or stimulated with IFNα for 15 min. **b**, Association of Flag- or HA-tagged wild-type (WT) and mutant STAT3s co-expressed in COS7 fibroblast cells was examined by immunoprecipitation (IP) with anti-HA or control antibody followed by immunoblotting (IB) with anti-Flag or HA antibody. **c**, DNA-binding activity of STAT3 and STAT1 in nuclear extracts prepared from EBV-LCLs from a healthy control and the HIES patients that were unstimulated or stimulated with IFNα for 15 min. Dark grey bars indicate the DNA-binding activity in the presence of competitor oligonucleotides, and black bars indicate non-specific binding to irrelevant oligonucleotides. Error bars are standard deviations.

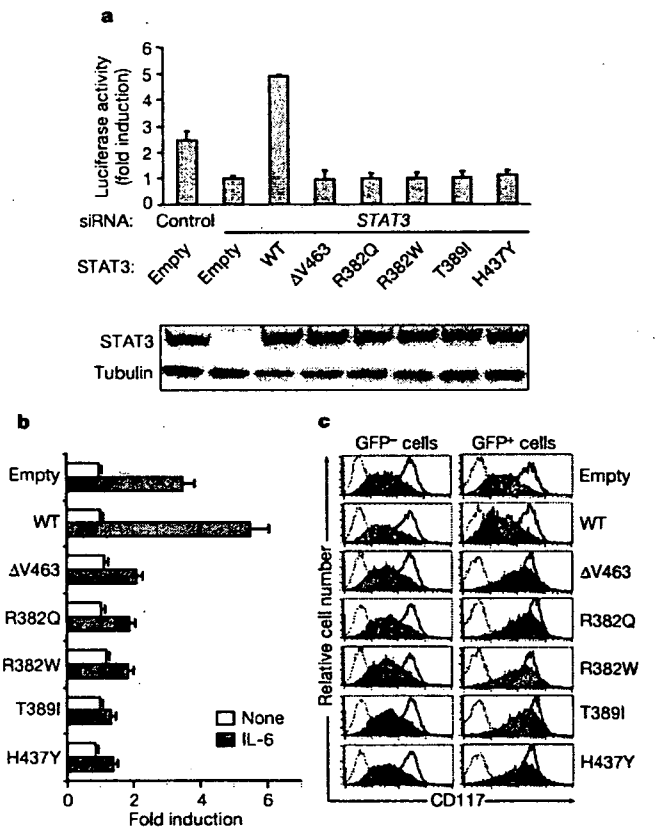

Figure 4 | Loss-of-function and dominant-negative effect of the STAT3 mutants in cytokine signals. **a**, Wild-type or individual mutants of STAT3 were exogenously expressed together with a luciferase reporter gene containing STAT3-responsive elements in human HeLa cells in which endogenous *STAT3* was knocked-down by transfecting with two sets of siRNA oligonucleotides. The HeLa cells were then left unstimulated or stimulated with 10 ng ml^{-1} of IFNα for 5 h. The relative luciferase activity in the cell lysates of IFNα-stimulated versus unstimulated cells is shown (error bars show standard deviations). Expression of endogenous and exogenous STAT3 proteins detected by immunoblotting is shown in the lower panel. **b**, The relative luciferase activity in the cell lysates of unstimulated or IL-6-stimulated HepG2 cells that were transfected with the luciferase reporter construct plus an empty vector or a vector containing the wild-type (WT) or one of each mutant *STAT3* sequence. Error bars show standard deviations. **c**, The CD117 expression level on untreated (thick line histograms) or IL-10-treated (shaded histograms) MC/9 cells that were infected with retroviral vectors containing WT or one of the mutant *STAT3* sequences. Data are shown for GFP$^+$ infected and GFP$^-$ uninfected cells, and thin dotted histograms indicate staining with a control antibody.

observed in HIES patients. Another remarkable feature of HIES is that patients are often afebrile and feel well[1], despite serious pneumonia or dermal pathology[4]. Indeed, acute-phase responses, such as an increase in serum C-reactive protein during severe infections, were diminished in our patients. STAT3 was originally identified as a protein binding to the IL-6-responsive element in the genes encoding hepatic acute-phase proteins[21,22], and the liver-specific inactivation of STAT3 leads to an impaired acute-phase response in mice[23]. Thus, the apparent lack of classical inflammatory responses in HIES patients could be attributed to defective signalling of pro-inflammatory cytokines, including IL-6.

Enhanced IgE production in the patients may reflect dysregulated immune responses owing to the impaired response to IL-10, a critical negative regulator[24], even though the exact mechanism of hyper IgE remains to be determined, as in the case of other disorders such as Wiskott-Aldrich syndrome. HIES patients often suffer from severe staphylococcal infection in the skin and lung. STAT3 plays a critical part in T_H17 development[25], and IL-17 produced by T_H17 cells is protective in the host defence against extracellular bacteria[26]. IL-22 stimulates cells in the skin and respiratory systems to produce β-defensins through STAT3 activation[27]. Thus, the susceptibility to bacterial infection could be attributed, at least in part, to the defects in T_H17 development and IL-22 signalling. Among the 15 sporadic HIES patients investigated in this study, no apparent difference was observed in clinical phenotypes and severity between those with the STAT3 mutations and those without the mutations, indicating that other HIES aetiology might be functionally linked to STAT3.

In summary, the present study identified a human deficiency in STAT3 as a major cause of multisystem HIES. This study highlights the multiple and critical roles of STAT3 in humans. The identification of these STAT3 mutations as causative for HIES, in addition to the previous finding of a causative mutation in TYK2 (ref. 8), underlines the critical involvement of a variety of cytokine signals in the pathogenesis of HIES. The diagnosis of HIES early in life is often hampered by a paucity of specific clinical features. Our discovery of STAT3 as a major causative gene of this disease will facilitate earlier and definitive diagnosis, leading to the prevention of serious complications by prompting the start of prophylactic antibiotic treatment early in life.

METHODS SUMMARY

Patients. This study was approved by the institutional review board at the Tokyo Medical and Dental University; written informed consent was obtained from all the individuals studied. The clinical characteristics of the eight HIES patients investigated in this study are summarized in Supplementary Table 1, and all the patients display definitive phenotypes of multisystem HIES (score ≥ 40).

Stimulation of cells with cytokines, and measurement of cytokines and IgM production. Cells were stimulated for the indicated time in culture with cytokines as described previously[8]. The concentration of IFNγ and TNFα in the culture supernatants was determined by ELISA (BD-PharMingen), according to the manufacturer's instructions. The amount of IgM secretion from EBV-infected B cells was determined as previously described[28].

RT–PCR and direct sequence analysis. Extraction of total RNA, cDNA synthesis, PCR, semiquantitative RT–PCR, and sequencing were performed as previously described[29].

Immunoblotting and immunoprecipitation. Immunoblotting and immunoprecipitation were performed as described previously[8].

Enzyme-linked DNA–protein interaction assay. Binding of STAT3 and STAT1 to their target DNA was measured using the Mercury TransFactor kit (Clontech Laboratories) according to the manufacturer's protocol.

Retroviral infections. Retroviral infections were done as described previously[8].

Flow cytometric analysis. The surface immunophenotype was analysed as described[30].

STAT3 knock-down. Transfection of short interfering RNA (siRNA) oligonucleotides (5′-ccugcaagagucgaauguucucuau-3′ and 5′-gcaguuucuucagagcaguaucuu-3′) was performed as described previously[8]. Forty hours after transfection, the cells were treated with IFNα for 5 h. In the experiment shown in Fig. 4a, nucleotide sequences of wild-type and mutant STAT3 cDNAs were modified so that they were insensitive to STAT3 siRNA, but they still encoded the original amino acid sequences of STAT3.

Luciferase reporter assay. The reporter construct of STAT3-responsive elements linked to a luciferase reporter gene was transfected with wild-type or mutant STAT3. Forty hours after the transfection, the cells were stimulated with 100 ng ml^{-1} IL-6 for 5 h. Luciferase activity was measured with a dual-luciferase assay system according to the manufacturer's protocol (Promega).

Full Methods and any associated references are available in the online version of the paper at www.nature.com/nature.

Received 28 June; accepted 19 July 2007.
Published online 5 August 2007; corrected 30 August 2007 (details online).

1. Grimbacher, B., Holland, S. M. & Puck, J. M. Hyper-IgE syndromes. *Immunol. Rev.* 203, 244–250 (2005).
2. Gould, H. J. *et al.* The biology of IGE and the basis of allergic disease. *Annu. Rev. Immunol.* 21, 579–628 (2003).
3. Grimbacher, B., Belohradsky, B. H. & Holland, S. M. Immunoglobulin E in primary immunodeficiency diseases. *Allergy* 57, 995–1007 (2002).
4. Davis, S. D., Schaller, J. & Wedgwood, R. J. Job's Syndrome. Recurrent, "cold", staphylococcal abscesses. *Lancet* 1, 1013–1015 (1966).
5. Buckley, R. H., Wray, B. B. & Belmaker, E. Z. Extreme hyperimmunoglobulinemia E and undue susceptibility to infection. *Pediatrics* 49, 59–70 (1972).
6. Grimbacher, B. *et al.* Hyper-IgE syndrome with recurrent infections—an autosomal dominant multisystem disorder. *N. Engl. J. Med.* 340, 692–702 (1999).
7. Renner, E. D. *et al.* Autosomal recessive hyperimmunoglobulin E syndrome: a distinct disease entity. *J. Pediatr.* 144, 93–99 (2004).
8. Minegishi, Y. *et al.* Human tyrosine kinase 2 deficiency reveals its requisite roles in multiple cytokine signals involved in innate and acquired immunity. *Immunity* 25, 745–755 (2006).
9. Schindler, C. & Darnell, J. E. Jr. Transcriptional responses to polypeptide ligands: the JAK-STAT pathway. *Annu. Rev. Biochem.* 64, 621–651 (1995).
10. Ihle, J. N. Cytokine receptor signalling. *Nature* 377, 591–594 (1995).
11. Levy, D. E. & Darnell, J. E. Jr. STATs: transcriptional control and biological impact. *Nature Rev. Mol. Cell Biol.* 3, 651–662 (2002).
12. Kisseleva, T., Bhattacharya, S., Braunstein, J. & Schindler, C. W. Signaling through the JAK/STAT pathway, recent advances and future challenges. *Gene* 285, 1–24 (2002).
13. Grimbacher, B. *et al.* Genetic linkage of hyper-IgE syndrome to chromosome 4. *Am. J. Hum. Genet.* 65, 735–744 (1999).
14. Horvath, C. M., Wen, Z. & Darnell, J. E. Jr. A STAT protein domain that determines DNA sequence recognition suggests a novel DNA-binding domain. *Genes Dev.* 9, 984–994 (1995).
15. Chapgier, A. *et al.* Novel *STAT1* alleles in otherwise healthy patients with mycobacterial disease. *PLoS Genet.* 2, e131 (2006).
16. Takeda, K. *et al.* Targeted disruption of the mouse *Stat3* gene leads to early embryonic lethality. *Proc. Natl Acad. Sci. USA* 94, 3801–3804 (1997).
17. Darnell, J. E. Jr. STATs and gene regulation. *Science* 277, 1630–1635 (1997).
18. Levy, D. E. & Lee, C. K. What does Stat3 do? *J. Clin. Invest.* 109, 1143–1148 (2002).
19. O'Brien, C. A., Gubrij, I., Lin, S. C., Saylors, R. L. & Manolagas, S. C. STAT3 activation in stromal/osteoblastic cells is required for induction of the receptor activator of NF-κB ligand and stimulation of osteoclastogenesis by gp130-utilizing cytokines or interleukin-1 but not 1,25-dihydroxyvitamin D3 or parathyroid hormone. *J. Biol. Chem.* 274, 19301–19308 (1999).
20. Itoh, S. *et al.* A critical role for interleukin-6 family-mediated Stat3 activation in osteoblast differentiation and bone formation. *Bone* 39, 505–512 (2006).
21. Akira, S. *et al.* Molecular cloning of APRF, a novel IFN-stimulated gene factor 3 p91-related transcription factor involved in the gp130-mediated signaling pathway. *Cell* 77, 63–71 (1994).
22. Zhong, Z., Wen, Z. & Darnell, J. E. Jr. Stat3: a STAT family member activated by tyrosine phosphorylation in response to epidermal growth factor and interleukin-6. *Science* 264, 95–98 (1994).
23. Li, W., Liang, X., Kellendonk, C., Poli, V. & Taub, R. STAT3 contributes to the mitogenic response of hepatocytes during liver regeneration. *J. Biol. Chem.* 277, 28411–28417 (2002).
24. Robinson, D. S., Larche, M. & Durham, S. R. Tregs and allergic disease. *J. Clin. Invest.* 114, 1389–1397 (2004).
25. Yang, X. O. *et al.* STAT3 regulates cytokine-mediated generation of inflammatory helper T cells. *J. Biol. Chem.* 282, 9358–9363 (2007).
26. Happel, K. I. *et al.* Divergent roles of IL-23 and IL-12 in host defense against *Klebsiella pneumoniae*. *J. Exp. Med.* 202, 761–769 (2005).
27. Wolk, K. *et al.* IL-22 increases the innate immunity of tissues. *Immunity* 21, 241–254 (2004).

28. Minegishi, Y. & Conley, M. E. Negative selection at the pre-BCR checkpoint elicited by human μ heavy chains with unusual CDR3 regions. *Immunity* 14, 631–641 (2001).
29. Minegishi, Y. *et al.* Mutations in Igα (CD79a) result in a complete block in B-cell development. *J. Clin. Invest.* 104, 1115–1121 (1999).
30. Minegishi, Y. *et al.* An essential role for BLNK in human B cell development. *Science* 286, 1954–1957 (1999).

Supplementary Information is linked to the online version of the paper at www.nature.com/nature.

Acknowledgements We appreciate the willingness of the patients and the families to participate in this research study. This work is supported by the Japanese Ministry of Education, Culture, Sports, Science and Technology, and the Japanese Ministry of Health, Labor and Welfare.

Author Contributions Y.M. designed and conducted most of the experiments; M.S. conducted the genetic analysis and the generation of osteoclasts; S.T., I.T., H.T., T.H., N.K., T.A., S.P. and A.M. diagnosed and collected samples; O.S. collected samples; H.K. oversaw the entire project; Y.M. and H.K. wrote the manuscript with comments from all co-authors.

Author Information Reprints and permissions information is available at www.nature.com/reprints. The authors declare no competing financial interests. Correspondence and requests for materials should be addressed to Y.M. (yminegishi.mbch@tmd.ac.jp).

METHODS

Patients. An immunological work-up revealed high serum IgE in all the patients and eosinophilia in five of them. All other laboratory data examined were within the normal range, including the lymphocyte subpopulations, their proliferative responses to mitogens, the levels and subclasses of serum immunoglobulins, the oxidative burst of granulocytes, and the number and size of platelets.

Antibodies and cytokines. Antibodies against STAT3, tyrosine-phosphorylated STAT3, Flag and HA, and HRP-conjugated rabbit anti-mouse and goat anti-rabbit antibodies were purchased from Cell Signaling. The CD117 monoclonal antibody was from BD-PharMingen, and the CD3 monoclonal antibody (OKT3) was from Janssen Pharmaceutical. Recombinant human IL-6, IL-10, IL-12, IFNα, and GM-CSF were purchased from Peprotech, recombinant human IL-2 from Shionogi, and lipopolysaccharide (055:B5) from Sigma-Aldrich.

Isolation and culture of T cells and macrophages from PBMCs. Isolation and cell culture of T cells and macrophages were performed as described previously[8]. All the experiments were performed at least three times with three different controls.

Stimulation of cells with cytokines, and measurement of cytokines and IgM production. Cells were stimulated for the indicated time in culture with IL-6 (100 ng ml^{-1}), IL-10 (100 ng ml^{-1}), IL-12 (10 ng ml^{-1}), or IFNα (5 ng ml^{-1}) as described previously[4].

RT–PCR and direct sequence analysis. Sequencing was performed with an ABI Prism dRhodamine Terminator kit and analysed with an ABI Prism 310 DNA Sequencer (Perkin-Elmer Applied Biosystems). At least two independent PCR products were sequenced.

Enzyme-linked DNA–protein interaction assay. Thirty micrograms of nuclear extracts were incubated in a 96-well microplate precoated with oligonucleotides encoding the consensus binding sequence for STAT1 or that for STAT3. Bound STAT3 or STAT1 was detected with specific antibodies plus an HRP-conjugated secondary antibody.

Retroviral infections. Retroviral infections were done with the retroviral vector pMX-IRES-GFP (a gift from T. Kitamura) carrying the wild-type or one of each mutant STAT3 sequence as described previously[8].

STAT3 knock-down. Transfection of siRNA oligonucleotides was performed by using Lipofectamine-RNAiMAX reagent (Invitrogen). Forty hours after transfection, the cells were treated with IFNα (10 ng ml^{-1}) for 5 h.

Luciferase reporter assay. The reporter construct contained 4 repeated STAT3-responsive elements linked to a luciferase reporter gene. HeLa cells or HepG2 cells were transfected with the pcDNA3 vector bearing wild-type or mutant *STAT3*, the reporter construct, and an expression vector for *Renilla* luciferase driven by the CMV reporter, with FuGENE6 (Roche). The relative luciferase activity was determined by normalizing the values against the *Renilla* luciferase signal.

H2-M3-Restricted CD8$^+$ T Cells Induced by Peptide-Pulsed Dendritic Cells Confer Protection against *Mycobacterium tuberculosis*[1]

Takehiko Doi,*† Hisakata Yamada,[2]* Toshiki Yajima,* Worawidh Wajjwalku,‡ Toshiro Hara,† and Yasunobu Yoshikai*

One of the oligopolymorphic MHC class Ib molecules, H2-M3, presents *N*-formylated peptides derived from bacteria. In this study, we tested the ability of an H2-M3-binding peptide, TB2, to induce protection in C57BL/6 mice against *Mycobacterium tuberculosis*. Immunization with bone marrow-derived dendritic cell (BMDC) pulsed with TB2 or a MHC class Ia-binding peptide, MPT64$_{190-198}$ elicited an expansion of Ag-specific CD8$^+$ T cells in the spleen and the lung. The number of TB2-specific CD8$^+$ T cells reached a peak on day 6, contracted with kinetics similar to MPT64$_{190-198}$-specific CD8$^+$ T cells and was maintained at an appreciable level for at least 60 days. The TB2-specific CD8$^+$ T cells produced less effector cytokines but have stronger cytotoxic activity than MPT64$_{190-198}$-specific CD8$^+$ T cells. Mice immunized with TB2-pulsed BMDC as well as those with MPT64$_{190-198}$-pulsed BMDC showed significant protection against an intratracheal challenge with *M. tuberculosis* H37Rv. However, histopathology of the lung in mice immunized with TB2-pulsed BMDC was different from mice immunized with MPT64$_{190-198}$-pulsed BMDC. Our results suggest that immunization with BMDC pulsed with MHC class Ib-restricted peptides would be a useful vaccination strategy against *M. tuberculosis*. *The Journal of Immunology*, 2007, 178: 3806–3813.

Tuberculosis is one of the major public health problems. About one-third of the world population has been latently infected with *Mycobacterium tuberculosis* (1). The tuberculosis incidence is increasing in association with increased numbers of HIV/AIDS patients. Furthermore, the emergency of multidrug-resistant strains of *M. tuberculosis* has worsened the problems. To prevent an epidemic of tuberculosis, *Mycobacterium bovis* bacillus Calmette-Guérin (BCG)[3] is the only vaccine currently available against tuberculosis. Although BCG vaccine protect children efficiently against the early manifestations of tuberculosis (2, 3), especially meningeal tuberculosis (4), it confers incomplete protection against tuberculosis in adults presumably because BCG may not be effective for inducing long-term cellular immunity sufficient for protection against pulmonary disease (5). Furthermore, BCG, a live vaccine, may not be safe for immunocompromised hosts such as AIDS and aged patients. Therefore, it is urgently required to develop prophylactic and therapeutic vaccines for tuberculosis in place of BCG (6).

Although protection against infection with intracellular bacteria such as *M. tuberculosis* depends mainly on CD4$^+$ Th1 cells, there are substantial lines of evidence that CD8$^+$ T cells also play a requisite role (7–9). β_2-microglobulin-deficient mice and TAP-deficient mice, both of which lack functional CD8$^+$ T cells, are susceptible to infection with *M. tuberculosis* (10, 11). Adoptive transfer of immunized CD8$^+$ T cells conferred protection against subsequent challenge with *M. tuberculosis* (12). Thereafter, various vaccination strategies have settled to efficiently induce protective memory CD8$^+$ T cells. Peptide-pulsed mature bone marrow-derived dendritic cells (BMDC) efficiently generate high numbers of effector and memory CD8$^+$ T cells (13–15) and there have been several studies on BMDC-based vaccines against *M. tuberculosis* (16–18) in which a certain level of protection was observed. However, an obstacle for clinical application of these peptide-based vaccination strategies is the polymorphism of MHC molecules (19).

Although most of CD8$^+$ T cells recognize peptides on highly polymorphic class Ia molecules, some CD8$^+$ T cells recognize peptides presented by class Ib molecules which have limited polymorphism (20). H2-M3 is a member of MHC class Ib molecules showing specificity for hydrophobic peptide sequences initiating with *N*-formyl methionine derived from only bacteria or mitochondrial proteins (21, 22). Chun et al. (23) have identified *M. tuberculosis*-derived peptides which bind H2-M3 and showed an involvement of H2-M3-restricted CD8$^+$ T cell response in murine models of *M. tuberculosis* infection. Thus, H2-M3-binding peptides may serve as a good candidate for universal vaccine against *M. tuberculosis* (24). At present, it is unclear whether immunization with H2-M3 peptide induces long-lasting protective immunity to *M. tuberculosis* infection.

In the present study, we examined the effects of vaccination with BMDC pulsed with a H2-M3-binding peptide, TB2 (23) or a MHC

*Division of Host Defense, Medical Institute of Bioregulation, Kyushu University, Fukuoka, Japan; †Department of Pediatrics, Faculty of Medicine, Kyushu University, Fukuoka, Japan; and ‡Department of Pathology, Faculty of Veterinary Medicine, Kasetsart University, Nakhonpathom, Thailand

Received for publication August 1, 2006. Accepted for publication January 10, 2007.

The costs of publication of this article were defrayed in part by the payment of page charges. This article must therefore be hereby marked *advertisement* in accordance with 18 U.S.C. Section 1734 solely to indicate this fact.

[1] This work was supported in part by the Program of Founding Research Centers for Emerging and Re-emerging Infectious Diseases launched as a project commissioned by the Ministry of Education, Culture, Sports, Science and Technology, Japan, by a Grant-in-Aid for Japan Society for Promotion of Science, and grants from the Japanese Ministry of Education, Science, and Culture (to Y.Y.).

[2] Address correspondence and reprint requests to Dr. Hisakata Yamada, Division of Host Defense, Medical Institute of Bioregulation, Kyushu University, Fukuoka 812-8582, Japan. E-mail address: hisaky@hotmail.com

[3] Abbreviations used in this paper: BCG, *Mycobacterium bovis* bacillus Calmette-Guérin; DC, dendritic cell; BMDC, bone marrow-derived DC; MFI, mean fluorescent intensity.

Table I. *Synthetic peptides used in this study*[a]

Peptide	Sequence and Location	Gene Designation and Putative Identification
MHC class Ia-restricted (H-2^b-restricted) peptide		
MPT64$_{190-198}$	FAVTNDGVI (190–198)	Rv1980c (immunogenic protein MPB64/MPT64)
Mtb32A$_{309-318}$	GAPINSATAM (309–318)	Rv0125 (probable serine protease PepA)
38 kDa$_{129-137}$	AQQVNYNLP (129–137)	Rv0934 (periplasmic phosphate-binding lipoprotein PSTS1)
OVA$_{257-264}$	SIINFEKL (257–264)	OVA
H2-M3-restricted peptide		
TB2	f-MLVLLV (1–6)	Rv0476 (possible conserved transmembrane protein)
TB4	f-MFLIDV (1–6)	Rv0277C (conserved hypothetical protein)
TB7	f-MILLV (1–5)	Rv1686C (probable conserved integral membrane protein ABC transporter)
LemA	f-MIGWII (1–6)	Listerial peptide

[a] The sequence and annotation information of *M. tuberculosis* was obtained from The Institute for Genomic Research (http://cmr.tigr.org/tigr-scripts/CMR/CmrHomePage.cgi) and The Institut Pasteur (http://genolist.pasteur.fr/TubercuList/).

class Ia (H-2D^b)- binding peptide, MPT64$_{190-198}$ (25–27) on *M. tuberculosis* H37Rv infection in mice. We found that immunization with TB2-pulsed BMDC elicited long-lasting Ag-specific CD8$^+$ T cells, leading to protection against intratracheal infection with *M. tuberculosis* at a level comparable to MPT64$_{190-198}$-pulsed BMDC.

Materials and Methods

Animals

Six- to 8-wk-old female C57BL/6 mice (Charles River Laboratories) and C57BL/6 Ly5.1-congenic mice (The Jackson Laboratory) were used. They were housed in a pathogen-free environment throughout the experiment. This study was approved by the Committee of Ethics on Animal Experiment in Faculty of Medicine (Kyushu University, Kyushu, Japan). Experiments were conducted under the control of the Guidelines for Animal Experiment and were performed mainly under barrier conditions in a level III biosafety animal facility.

Microorganisms

M. tuberculosis strain H37Rv was grown in Middlebrook 7H9 medium (Difco) supplemented with albumin-dextrose-catalase enrichment (Difco) and Tween 80 at 37°C. The bacteria in the culture were stored in Middlebrook 7H9 medium supplemented with 20% (v/v) glycerol at −80°C until they were used.

Abs and synthetic peptides

Following Abs were used: FITC-conjugated anti-IFN-γ (R4-6A2), Cy5-conjugated anti-CD8a (53-6.7), PE-conjugated anti-CD44 (IM7), biotin-conjugated anti-CD45.1 (A20), and streptavidin-Cy5 (eBioscience). The H2-D^b-restricted peptide, MPT64$_{190-198}$ (FAVTNDGVI) (25–27), Mtb32A$_{309-318}$ (GAPINSATAM) (28, 29), 38 kDa$_{129-137}$ (AQQVNY NLP) (30), the H2-K^b-restricted peptide, OVA$_{257-264}$ (SIINFEKL), and the H_2-M_3-restricted peptide, TB2 (f-MLVLLV), TB4 (f-MFLIDV), TB7 (f-MILLV) (23), and LemA (f-MIGWII) (Table I) were purchased from Greiner Bio-One.

Generation of peptide-pulsed BMDCs and immunization

RBC-depleted bone marrow cells were cultured at 1 × 10^6 cells/ml in RPMI 1640 medium (Sigma-Aldrich) supplemented with 20 ng/ml murine IL-4 and 20 ng/ml murine GM-CSF (PeproTech) at 37°C with 5% CO_2. Three days after the initial culture, two-thirds of the medium containing small nonadherent cells were removed and fresh RPMI 1640 containing GM-CSF and IL-4 was added back. At day 6, 1 μg/ml LPS (Sigma-Aldrich) was added to induce maturation. After an overnight culture, 5 μM synthetic peptides are added to the cultures 3 h before harvest. The nonadherent cells were harvested and then layered onto 15% metrazimade (Sigma-Aldrich). After a centrifugation at 600 × *g* for 20 min at 20°C, mononuclear cells at the interface were collected and washed twice before immunization. These cells were 80–90% CD11c$^+$ and expressed high levels of CD80, CD86, CD40 molecules. C57BL/6 mice were injected i.v. with 1 × 10^6 peptide-pulsed BMDC via the dorsal tail vein. Control mice received either PBS or none peptide-pulsed BMDC.

Quantification of Ag-specific CD8$^+$ T cell response

The number of CD8$^+$ T cells specific for MPT64$_{190-198}$ or TB2 was determined by intracellular staining for IFN-γ. The cells were incubated for 5–6 h with or without 5 μM of synthetic peptides in the presence of 10 μg/ml brefeldin A at 37°C. For the surface staining, cells were first incubated with a mAb directed against the Fcγ II/III receptors (2.4G2) and were incubated with PE-conjugated anti-CD44 mAb and Cy5-conjugated anti-CD8 mAb. The cells were fixed, permeabilized, and further stained with FITC-conjugated anti-IFN-γ mAb. Samples were run on a FACSCalibur flow cytometer (BD Biosciences) and analyzed with CellQuest software (BD Biosciences).

Quantification of cytokine by ELISA

CD8$^+$ T cells in the spleens were purified after depleting nylon wool-adherent cells by positive selection using anti-CD8 magnetic beads (Miltenyi Biotec). CD8$^+$ T cells (2 × 10^5) were cocultured with mitomycin C-treated syngeneic splenocytes (2 × 10^5) from naive C57BL/6 mice at a volume of 200 μl in the presence or absence of different concentrations of synthetic peptides. The cells were incubated at 37°C and 5% CO_2 for 48 h and culture supernatants were collected and stored at −20°C. The amount of IFN-γ and TNF-α was measured by ELISA kit (R&D Systems) according to the manufacturer's protocols.

In vivo cytotoxicity assay

B6-Ly5.1$^+$ splenocytes were divided and labeled with either a high concentration (5 μM) or a low concentration (0.5 μM) of CFSE (Invitrogen Life Technologies). CFSE^{high} cells were pulsed with 5 μM synthetic peptide for 1 h at 37°C, whereas CFSE^{low} cells left uncoated. After washing, the cells were mixed in equal proportions (2 × 10^7 total cells/200 μl) and injected i.v. into mice immunized with peptide-pulsed DC 6 days previously. Splenocytes in the recipients were harvested 4 h later for flow cytometric analysis. Percent-specific lysis was calculated according to the formula (1 − (ratio primed/ratio unprimed) × 100), where the ratio unprimed = percent CFSE^{low}/percent CFSE^{high} cells remaining in nonimmunized recipients, and ratio primed = percent CFSE^{low}/percent CFSE^{high} cells remaining in immunized recipients.

Infection of immunized mice with M. tuberculosis

Mice were anesthetized by i.p. injection of pentobarbital sodium and tracheae were exposed. Infection was effected by intratracheal inoculation with 1 × 10^5 viable CFU of *M. tuberculosis* H37Rv diluted in 50 μl of PBS. The numbers of viable bacteria in organs were measured 7 or 28 days after infection by plating serial dilutions of whole organ homogenates on supplemented Middlebrook 7H10 agar (Difco) enriched with 10% oleic acid-albumin-dextrose-catalase (Difco) and 0.5% glycerol, and incubated at 37.5°C for 3 wk. Colonies were counted and total tissue CFU calculated.

ELISPOT assay

The numbers of MPT64$_{190-198}$- or TB2-specific T cells in the lungs and spleen after infection with *M. tuberculosis* were determined by an ELISPOT assay (Mouse IFN-γ ELISPOT Set; BD Biosciences) according to the manufacturer's instructions. Lung mononuclear cells were prepared by collagenase digestion and were pooled from three mice. To supplement

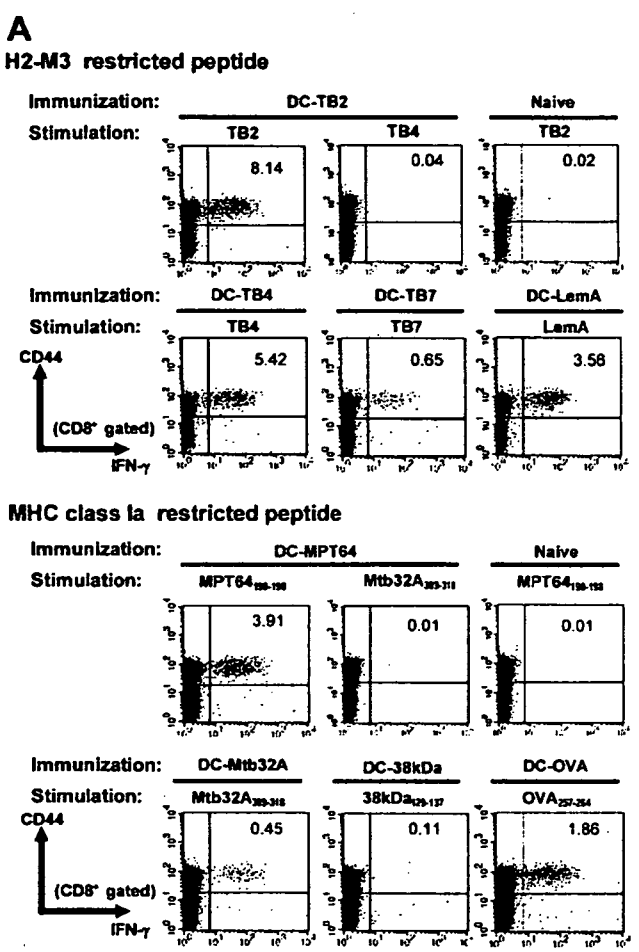

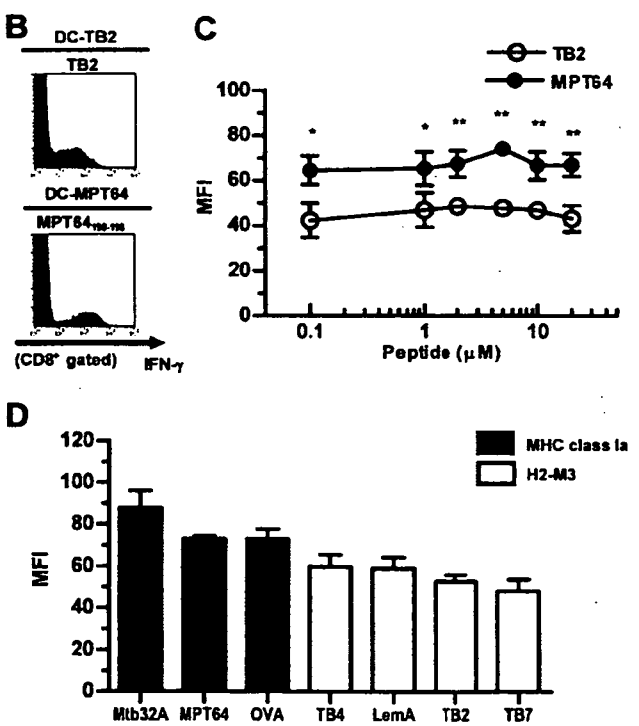

FIGURE 1. Expansion of Ag-specific $CD8^+$ T cells after immunization with *M. tuberculosis*-derived peptide-pulsed BMDCs. *A*, $CD8^+$ T cells in the spleens of naive mice or the mice immunized with H2-M3 (*upper panels*) or MHC class Ia (*lower panels*) restricted peptide-pulsed BMDCs 6 days previously were harvested and restimulated with the indicated peptide in vitro. IFN-γ-producing $CD8^+$ T cells were detected by a flow cytometer. Data are representative of three separate experiments and are expressed as means of three mice in each group. DC-MPT64, $MPT64_{190-198}$-pulsed BMDC; DC-Mtb32, $Mtb32A_{309-318}$-pulsed BMDC; DC-38 kDa, 38-$kDa_{129-137}$-pulsed BMDC; DC-OVA, $OVA_{257-264}$-pulsed BMDC; DC-TB2, TB2-pulsed BMDC; DC-TB4, TB4-pulsed BMDC; DC-TB7, TB7-pulsed BMDC; DC-LemA, LemA-pulsed BMDC. *B*, Expression levels of intracellular IFN-γ of TB2-specific $CD8^+$ T cells (*upper panel*) and $MPT64_{190-198}$-specific $CD8^+$ T cells (*lower panel*) were depicted as histograms. *C*, MFI of IFN-γ staining of $CD8^+$ T cells induced by different concentrations of peptide was shown. Data are representative of three separate experiments and are expressed as means + SD of three mice in each group. *, $p < 0.05$, **, $p < 0.01$, significantly different from the value of TB2-specific $CD8^+$ T cells. *D*, MFI of IFN-γ staining of $CD8^+$ T cells induced by different peptides was shown. Data are representative of three separate experiments and are expressed as means + SD of three mice in each group.

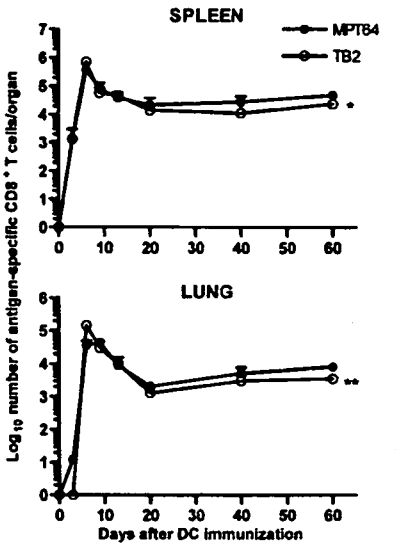

FIGURE 2. Kinetics of the absolute number of $MPT64_{190-198}$-specific or TB2-specific, IFN-γ-producing $CD8^+$ T cells in the spleens and the lungs. To calculate the number of Ag-specific $CD8^+$ T cells, we subtracted the percentage of IFN-γ^+ $CD8^+$ T cells in unstimulated samples from the peptide-stimulated value. Data are representative of three separate experiments and are expressed as means + SD of three mice in each group. *, $p < 0.05$, significantly different from the value of $MPT64_{190-198}$-specific $CD8^+$ T cells.

APCs in the lung cells, mitomycin C-treated syngeneic splenocytes were added at a ratio of 1:1 lung cells/APCs. Two-fold serial dilutions of the 100-μl admixture were added in triplicate to the wells precoated with anti-mouse IFN-γ mAb starting at 1×10^5 lung cells/well. The wells were further added with 100 μl of RPMI 1640-FCS containing no Ag, 5 μM $MPT64_{190-198}$ or 5 μM TB2. After 24 h of incubation at 37°C and 5% CO_2, unattached cells were aspirated from the wells and the remaining cells were lysed with distilled water. The wells were washed again with PBS containing 0.05% Tween 20 and incubated with a second biotinylated anti-mouse IFN-γ mAb. The wells were then washed with PBS-Tween 20, incubated for 1 h with streptavidin-HRP, washed, and developed with 3-amino-9-ethyl-carbazol as substrate. After washing and drying, the number of spots per well was counted with the aid of a digital microscope at ×40. The number of cells specific for each peptide was calculated by subtracting the number of spots formed in the absence of Ag from that formed in its presence. Experiments were repeated twice.

Histopathology

Tissues were preserved in 10% buffered formalin, embedded in paraffin, sectioned, and stained with H&E. Random sections including hilar of the lung from five mice per group were examined.

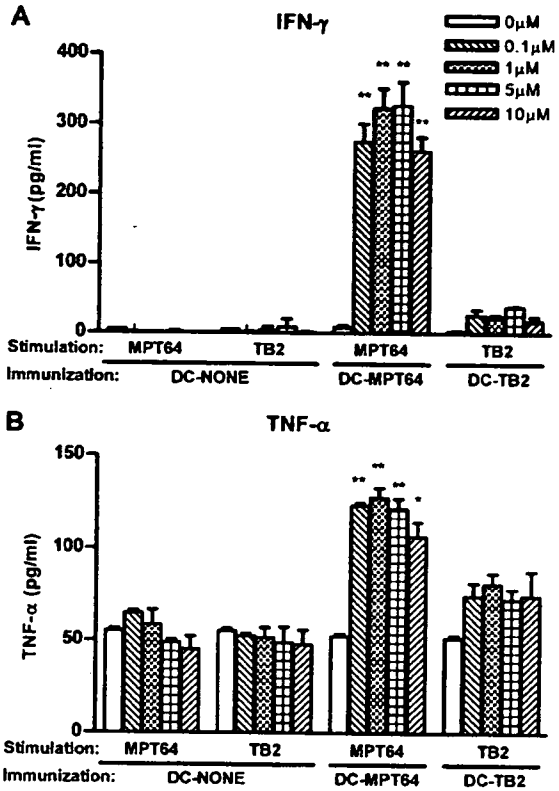

FIGURE 3. Cytokine production by $MPT64_{190-198}$- or TB2-specific $CD8^+$ T cells. Mice were immunized with $MPT64_{190-198}$ (DC-MPT64), TB2 (DC-TB2), or no peptide-pulsed BMDC (DC-NONE). After 6 days, purified $CD8^+$ T cells from the spleens were cultured with PBS or different concentrations of $MPT64_{190-198}$ or TB2 and syngeneic mitomycin C-treated splenocytes for 48 h. IFN-γ (*A*) and TNF-α (*B*) in the supernatants was measured by ELISA. Data are representative of three separate experiments and are expressed as means + SD of triplicate cultures of each group. *, $p < 0.05$, **, $p < 0.01$, significantly different from the value of TB2- specific $CD8^+$ T cells.

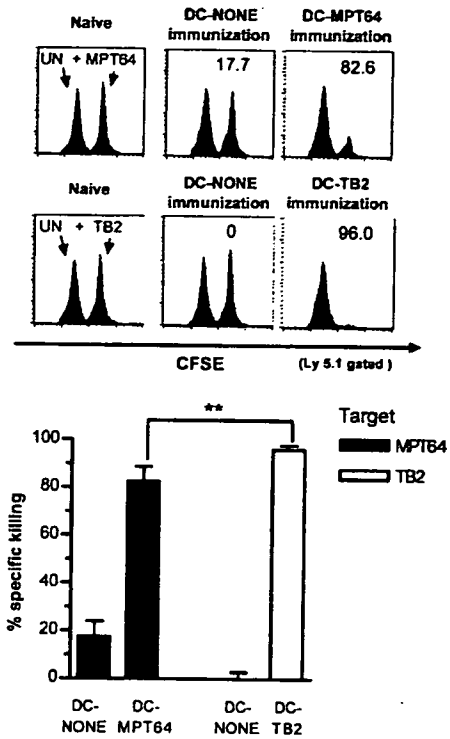

FIGURE 4. In vivo cytotoxic activity of $MPT64_{190-198}$- or TB2-specific $CD8^+$ T cells. Mice were immunized with $MPT64_{190-198}$ (DC-MPT64), TB2 (DC-TB2), or no peptide-pulsed BMDC (DC-NONE). Six days after immunization, CFSE-labeled, $MPT64_{190-198}$-, or TB2-pulsed and untreated (UN) target splenocytes ($Ly5.1^+$) were coinjected. Cytotoxic activity was expressed as the percent of specific killing of the targets. Data are representative of three separate experiments and are expressed as means + SD of four mice in each group. **, $p < 0.01$ significantly different from the value of $MPT64_{190-198}$-specific $CD8^+$ T cells.

Statistical analysis

The statistical significance of the bacteria number was determined by one-way ANOVA. Other data were determined by the Student *t* test. Differences with a *p* value of <0.05 were considered significant. Analyses were completed using SPSS software.

Results

Induction of MHC class Ia- and H2-M3-restricted $CD8^+$ T cell expansion by peptide-pulsed BMDCs

Chun et al. (23) have identified several *M. tuberculosis*-derived peptides binding to a MHC class Ib molecule, H2-M3. We first compared immunogenicity of three of these peptides named TB2, TB4, and TB7 (Table I), all of which were shown to be immunogenic in *M. tuberculosis*-infected C57BL/6 mice (23). We examined expansion of Ag-specific T cells after immunization with peptide-pulsed BMDC, which were treated with LPS to induce full maturation. We found this maturation step was necessary for inducing clear expansion of Ag-specific T cells in preliminary experiments (data not shown). As shown in Fig. 1*A*, an expansion of $CD8^+$ T cells producing IFN-γ was observed 6 days after immunization with H2-M3-binding peptides. Among the peptides tested, TB2 induced the strongest expansion of Ag-specific T cells. We also tested three MHC class Ia-restricted peptides derived from *M. tuberculosis* (Table I) for their immunogenicity. Although $MPT64_{190-198}$ gave a strong T cell response similar to the control OVA, the other two *M. tuberculosis*-derived peptides induced only marginal expansion of Ag-specific T cells. Therefore, we used TB2 and $MPT64_{190-198}$ as representative of H2-M3-binding and MHC class Ia-binding peptides, respectively, in the subsequent experiments. It is of note to find that, mean fluorescent intensity (MFI) for IFN-γ staining of $MPT64_{190-198}$-specific $CD8^+$ T cells was higher than that of TB2-specific $CD8^+$ T cells at any concentration of the peptides (Fig. 1, *B* and *C*). Furthermore, $CD8^+$ T cells specific for MHC class Ia-restricted peptides generally showed higher MFI than those specific for H2-M3-binding peptide (average MFI 77.8 vs 55.0, respectively, $p = 0.007$) (Fig. 1*D*).

Kinetic analysis revealed that the number of $MPT64_{190-198}$- or TB2-specific $CD8^+$ T cells in the spleen and the lung peaked on day 6 after immunization and contracted until day 20, and then was maintained an appreciable level at least 60 days (Fig. 2). The absolute number of TB2-specific $CD8^+$ T cells tended to be higher than that of $MPT64_{190-198}$-specific $CD8^+$ T cells in the spleen at the peak, but there were no significant differences. Although the number of TB2-specific $CD8^+$ T cells was lower than that of $MPT64_{190-198}$-specific $CD8^+$ T cells at day 60, it was still above background. These data showed that not only MHC class Ia-restricted $MPT64_{190-198}$- but also H2-M3-restricted TB2-pulsed mature BMDC induced long-lasting Ag-specific $CD8^+$ T cells.

Effector functions of TB2- and MPT64-specific $CD8^+$ T cells

As potential of IFN-γ production seemed different between MHC class Ia- and H2-M3-restricted $CD8^+$ T cells by intracellular flow

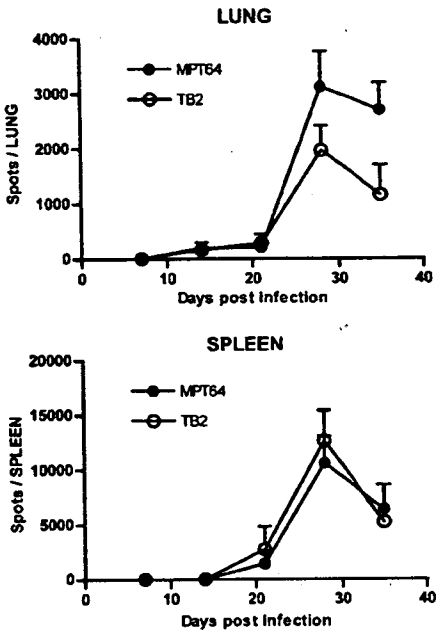

FIGURE 5. Kinetics of the number of $MPT64_{190-198}$- or TB2-specific $CD8^+$ T cells in *M. tuberculosis*-infected mice. Mice were infected intratracheally with 2×10^2 CFU *M. tuberculosis*. Number of $CD8^+$ T cells producing IFN-γ in response to $MPT64_{190-198}$ or TB2 per organ was measured by an ELISPOT assay. Results were obtained with pooled lung and spleen cells from three mice. Shown are the means + SD of the number of spots in triplicate wells. Similar results were obtained in two separate experiments.

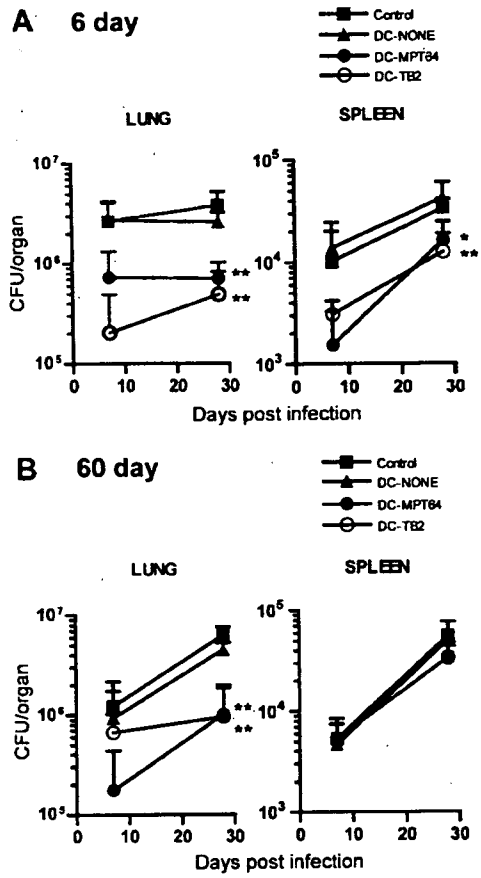

FIGURE 6. Protection against virulent *M. tuberculosis* H37Rv by immunization with $MPT64_{190-198}$ or TB2. Mice were immunized with BMDC pulsed with $MPT64_{190-198}$ (DC-MPT64), TB2 (DC-TB2), or no peptide (DC-NONE). Control mice were given PBS alone. At 6 days (*A*) or 60 days (*B*) postimmunization, the mice were challenged intratracheally with 1×10^5 CFU of live *M. tuberculosis* H37Rv. Data are representative of two separate experiments and are expressed as means + SD of four mice of each group. *, $p < 0.05$, **, $p < 0.01$ significantly different from the values of PBS and DC-NONE-immunized mice.

cytometric analysis (Fig. 1, *B–D*), we further compared the functions of TB2-specific $CD8^+$ T cells and $MPT64_{190-198}$-specific $CD8^+$ T cells 6 days after immunization. IFN-γ and TNF-α production by spleen $CD8^+$ T cells were measured by ELISA. Although there was no significant difference between the number of TB2-specific $CD8^+$ T cells and that of $MPT64_{190-198}$-specific $CD8^+$ T cells in the spleen as shown in Fig. 2, TB2-specific $CD8^+$ T cells produced less IFN-γ than $MPT64_{190-198}$-specific $CD8^+$ T cells at any concentration of the peptide (Fig. 3*A*). The level of TNF-α production was also lower in TB2-specific $CD8^+$ T cells than $MPT64_{190-198}$-specific $CD8^+$ T cells (Fig. 3*B*).

We next evaluated the cytotoxic activity of $MPT64_{190-198}$- or TB2-specific $CD8^+$ T cells by measuring in vivo cytotoxic activity against syngeneic peptide-pulsed splenocytes 6 days after immunization. Both $MPT64_{190-198}$-specific $CD8^+$ T cells and TB2-specific $CD8^+$ T cells lysed peptide-pulsed syngeneic splenocytes (Fig. 4). As opposed to the case of IFN-γ or TNF-α production, the cytotoxic activity of TB2-specific $CD8^+$ T cells was significantly higher than that of $MPT64_{190-198}$-specific $CD8^+$ T cells. Taken together, these data indicated that, although H2-M3-restricted TB2-specific $CD8^+$ T cells and MHC class Ia-restricted $MPT64_{190-198}$-specific $CD8^+$ T cells expand in similar extent with similar time kinetics after immunization with BMDC, they have somewhat different activities of function.

Response of $MPT64_{190-198}$- or TB2-specific $CD8^+$ T cells during infection with M. tuberculosis

To examine whether $CD8^+$ T cell response to $MPT64_{190-198}$ or TB2 was elicited during infection with *M. tuberculosis*, the number of $MPT64_{190-198}$- or TB2-specific T cells in the lung or spleen from 2×10^2 CFU *M. tuberculosis* H37Rv-infected mice was measured by an ELISPOT assay (Fig. 5). Two weeks after infection, a small number of peptide-specific IFN-γ spots was detected in the lung and the spleen. The frequency of $MPT64_{190-198}$- and TB2-specific $CD8^+$ T cells both rapidly increased from 3 wk after infection then reached a peak at 4 wk after infection. These results clearly indicate that $MPT64_{190-198}$ and TB2 are presented during *M. tuberculosis* infection. There was no clear difference in kinetics of the response between $MPT64_{190-198}$- and TB2-specific $CD8^+$ T cells.

H2-M3-restricted TB2-specific $CD8^+$ T cells protect mice from intratracheal M. tuberculosis *infection*

To examine whether these $CD8^+$ T cells are both protective against *M. tuberculosis*, we challenged the mice intratracheally with *M. tuberculosis* H37Rv 6 days after immunization with $MPT64_{190-198}$-pulsed BMDC (DC-MPT64), TB2-pulsed BMDC (DC-TB2), or BMDC without peptides (DC-NONE) (Fig. 6*A*). One or 4 wk after infection, lungs and spleens were prepared from the mice and the extent of bacterial growth was determined. At 1 wk, the CFU in the lung of DC-TB2-immunized mice tended to be lower than those of DC-NONE-immunized mice or naive mice, but it was not statistically significant. At 4 wk, the CFU in these organs of DC-MPT64 or DC-TB2 immunized mice was significantly lower than that of DC-NONE-immunized mice or naive mice. The

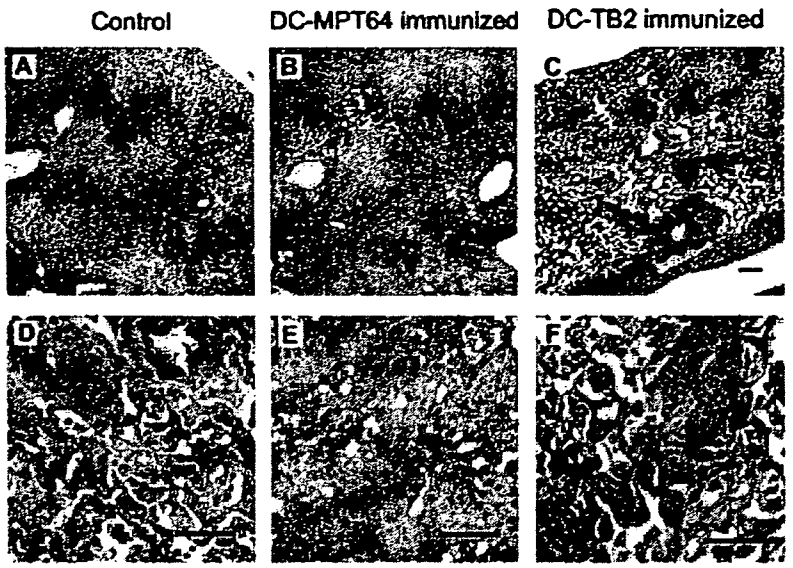

FIGURE 7. Lung histopathology of the mice immunized with $MPT64_{190-198}$- or TB2-pulsed BMDC following *M. tuberculosis* infection. Control PBS-injected mice (*A* and *D*) or the mice immunized with BMDC pulsed with $MPT64_{190-198}$ (DC-MPT64) (*B* and *E*) or TB2 (DC-TB2) (*C* and *F*) were challenged intratracheally with *M. tuberculosis*. After 8 wk, histology of the lungs was examined by staining with H&E. Lungs from five mice per group were examined. Representative figures are shown. Original magnification, ×4, scale length, 100 μm (*A–C*); ×20, scale length, 50 μm (*D–F*).

difference of the CFU in the lung was ~1 log10 order. Thus, both $MPT64_{190-198}$-specific $CD8^+$ T cells and TB2 specific-$CD8^+$ T cells were protective against respiratory *M. tuberculosis* infection.

Vaccination with TB2-pulsed BMDC conferred long-lasting protective immunity against M. tuberculosis

As shown in Fig. 2, $MPT64_{190-198}$-specific $CD8^+$ T cells and TB2-specific $CD8^+$ T cells were maintained for 60 days after immunization. To evaluate whether BMDC immunization can induce long-lasting protective immunity against *M. tuberculosis*, we challenged intratracheally with *M. tuberculosis* 60 days later after immunization. At 4 wk, the CFU in the lungs of DC-MPT64- or DC-TB2-immunized mice was significantly lower than those of DC-NONE-immunized mice and naive mice (Fig. 6*B*). The difference of the CFU in the lungs was ~1 $\log_{10}$ order. Although the CFU in the spleens was considerably lower than that of DC-NONE-immunized mice or naive mice, there was no statistical difference. These data suggested that both MHC class Ia-restricted $CD8^+$ T cells and H2-M3-restricted $CD8^+$ T cells induced by peptide-pulsed mature BMDC elicited long-lasting protection against respiratory *M. tuberculosis* infection.

Lung histopathology of the mice immunized with TB2 or $MPT64_{190-198}$ *after intratracheal* M. tuberculosis *infection*

As we observed some differences in the activity of function between $MPT64_{190-198}$- and TB2-specific $CD8^+$ T cells in vivo as well as in vitro (Figs. 3 and 4), it is of interest to compare histopathological changes in the lungs of the mice immunized with the different peptides. DC-MPT64-immunized mice had larger pulmonary infiltrates composed of formed macrophages (Fig. 7, *B* and *E*) compared with control (Fig. 7, *A* and *D*) or DC-TB2-immunized mice (Fig. 7, *C* and *F*). Areas of bronchopneumonia were clearly evident and frankly necrotic areas were observed in part (Fig. 7*B*). In contrast, although large infiltrates were also observed in the lungs of DC-TB2-immunized mice, there were few necroses and the structure of the walls of the alveoli comparatively avoided destruction (Fig. 7*C*). There tended to be greater numbers of lymphocytes in the inflammatory infiltrate compared with DC-MPT64-immunized mice. Both perivascular and interstitial lymphoid infiltrates were observed (Fig. 7*F*). These histopathological features suggest that the protection mechanism of TB2-specific $CD8^+$ T cells against *M. tuberculosis* infection is different from that of $MPT64_{190-198}$-specific $CD8^+$ T cells.

Discussion

Because $CD8^+$ T cells play a requisite role in the resistance to mycobacterial infection, Ag-specific $CD8^+$ T cells are major target for vaccine design for tuberculosis. We here showed the first evidence that immunization with mature BMDC pulsed with either MHC class Ia ($H\text{-}2D^b$) binding $MPT64_{190-198}$ or class Ib (H2-M3) binding TB2 peptide induced long-lasting Ag-specific $CD8^+$ T cells and conferred protection against an intratracheal challenge with *M. tuberculosis*.

There have been several studies on BMDC-based vaccination against *M. tuberculosis* infection models in mice (16–18). McShane et al. (18) reported that mice immunized with immature BMDC pulsed with either MHC class I- or MHC class II-restricted Ag85A peptide was not protective against *M. tuberculosis* challenge. Nakano et al. (16) reported that retroviral *Ag85A* gene-transduced, incompletely matured BMDC immunization was not effective enough in terms of clearance of *M. tuberculosis* from the tissues. In contrast, Malowany et al. (17) reported that adenoviral *Ag85A* gene-transduced mature BMDC induced much longer immune response compare with immature peptide-pulsed BMDC. These findings clearly indicated the importance of maturational stage of BMDC for vaccination. We also observed a clear difference in inducing T cell response between immature and mature BMDC (data not shown). Thereafter, we used LPS-stimulated BMDC for immunization and successfully induced protective $CD8^+$ T cell responses against *M. tuberculosis* infection.

There have been some reports showing an involvement of H2-M3-restricted $CD8^+$ T cells in *M. tuberculosis* infection. Chun et al. (23) identified several H2-M3-binding peptides by scanning the full sequence of the *M. tuberculosis* genome. Although they showed $CD8^+$ T cell responses to some of these peptides including TB2 after infection with *M. tuberculosis*, it has been unknown whether the H2-M3-restricted $CD8^+$ T cells are protective against *M. tuberculosis* infection. Dow et al. (31) also identified several H2-M3-binding peptides derived from *M. tuberculosis* and showed CTL response to these peptides. They also examined protection against *M. tuberculosis* challenged 10 days after immunization with some of these peptides. However, these peptides were longer

than the predicted length of H2-M3-binding peptides revealed by the crystallography (32) and also by bioassays (33), and none of these peptides were identical with the peptides identified by Chun et al. (23). In this study, we found TB2 elicited strongest T cell response after immunization with peptide-pulsed BMDC. Thereafter, we used TB2 and found that immunization with TB2 confers significant protection as vaccine against *M. tuberculosis* challenged even 60 days after immunization.

The importance of H2-M3-restricted $CD8^+$ T cells has been more clearly shown in *Listeria monocytogenes* infection. It was recently reported that H2-M3-deficient mice were impaired in early bacterial clearance during primary *L. monocytogenes* infection (34). H2-M3-restricted $CD8^+$ T cells play a role in early protection against a primary *L. monocytogenes* infection by expanding quicker than class Ia-restricted $CD8^+$ T cells (35, 36). In the present study, however, we did not find difference in the kinetics of expansion between H2-M3-restricted $CD8^+$ T cells and MHC class Ia-restricted $CD8^+$ T cells either after immunization with BMDC or during *M. tuberculosis* infection. In the former case, the discrepancy between the previous observations and our findings may be explained by different efficacy in Ag processing between MHC class Ia-binding peptides and H2-M3-binding peptides. For the presentation by MHC class Ia molecules, antigenic peptides in the cytosol are translocated to the lumen of the endoplasmic reticulum by TAP and loaded onto peptide-receptive MHC class Ia complexes. Stably conformed and peptide-filled class Ia complexes then egress from the endoplasmic reticulum to the cell surface. In contrast, TAP did not appear to be absolutely necessary for the presentation of *N*-formylated peptides by H2-M3 molecules (37). In addition, the supply of endogenous *N*-formylated mitochondrial peptides is limited and a significant pool of H2-M3 exists intracellularly, which can be rapidly mobilized to the surface when provided with appropriate exogenous *N*-formylated peptides (38). Therefore, it is suggested that MHC class Ib-binding Ag peptides are more rapidly presented by APCs. Immunization with peptide-pulsed mature BMDC may circumvent these time-dependent factors. In the case of in vivo infection, one of the major differences between *L. monocytogenes* and *M. tuberculosis* is their growth rate. *M. tuberculosis* divide slowly and their Ags are presented gradually with time, which may conceal the lag of response of MHC class Ia-restricted $CD8^+$ T cells behind that of H2-M3-restricted $CD8^+$ T cells. Additionally, there seems to be a difference in Ag processing between *L. monocytogenes* and *M. tuberculosis*. In contrast to *L. monocytogenes*, which actively escapes phagosomes and enters the cytosol, *M. tuberculosis* resides within phagosomes which has features similar to those of an early endosome (39, 40). Nevertheless, *M. tuberculosis*-derived peptides are cross-presented by MHC class I pathway, which is supposed to be far less efficient than the case of *L. monocytogenes*. These differences in Ag processing and presentation of different microbes may also be involved in the discrepancy.

There were some differences in the activities of effector functions between H2-M3-restricted TB2-specific $CD8^+$ T cells and MHC class Ia-restricted $MPT64_{190-198}$-specific $CD8^+$ T cells, although both were protective against *M. tuberculosis* infection. Cytotoxic activity of TB2-specific $CD8^+$ T cells was higher than that of $MPT64_{190-198}$-specific $CD8^+$ T cells, whereas the ability to produce IFN-γ or TNF-α was the opposite. Such differences are usually observed after immunization with different peptides, even restricted by the same MHC molecule and could be related to the stability of the MHC complexes. In this regard, it is notable to find that the expression levels of IFN-γ were generally lower in H2-M3-restricted $CD8^+$ T cells than in MHC class Ia-restricted $CD8^+$ T cells by intracellular flow cytometric analysis (Fig. 1*D*), suggesting that the difference in the activities of function between TB2- and $MPT64_{190-198}$-specific $CD8^+$ T cells may be generalized to difference between MHC class Ia- and MHC class Ib-restricted $CD8^+$ T cells. Further detailed analysis is needed to test this possibility. These differences in activities of function of $CD8^+$ T cells might result in the different histopathology of the lung between $MPT64_{190-198}$- and TB2-immunized mice. The lungs of $MPT64_{190-198}$-pulsed BMDC-immunized mice following *M. tuberculosis* infection had large pulmonary infiltrates composed of formed macrophages. In contrast, the lungs of TB2-pulsed BMDC-immunized mice following *M. tuberculosis* infection had less necrosis and reduced pulmonary injury.

In conclusion, our results clearly indicated that vaccination with mature BMDC pulsed with a H2-M3-binding peptide significantly confers protection against *M. tuberculosis*. Because MHC class Ib molecules including H2-M3 have an advantage of limited polymorphism, immunization with MHC class Ib-restricted peptides would be a novel vaccination strategy against *M. tuberculosis* infection for a broad range of recipients.

Acknowledgments

We thank Kazue Hirowatari and Yoko Tagawa for their excellent technical assistance.

Disclosures

The authors have no financial conflict of interest.

References

1. Dye, C., S. Scheele, P. Dolin, V. Pathania, and M. C. Raviglione. 1999. Consensus statement: global burden of tuberculosis: estimated incidence, prevalence, and mortality by country. WHO Global Surveillance and Monitoring Project. *J. Am. Med. Assoc.* 282: 677–686.
2. Lancksriet, C., D. Levy-Bruhl, E. Bingono, R. M. Siopathis, and N. Guerin. 1995. Efficacy of BCG vaccination of the newborn: evaluation by a follow-up study of contacts in Bangui. *Int. J. Epidemiol.* 24: 1042–1049.
3. Colditz, G. A., C. S. Berkey, F. Mosteller, T. F. Brewer, M. E. Wilson, E. Burdick, and H. V. Fineberg. 1995. The efficacy of bacillus Calmette-Guerin vaccination of newborns and infants in the prevention of tuberculosis: meta-analyses of the published literature. *Pediatrics* 96: 29–35.
4. Mittal, S. K., V. Aggarwal, A. Rastogi, and N. Saini. 1996. Does B.C.G. vaccination prevent or postpone the occurrence of tuberculous meningitis? *Indian J. Pediatr.* 63: 659–664.
5. Colditz, G. A., T. F. Brewer, C. S. Berkey, M. E. Wilson, E. Burdick, H. V. Fineberg, and F. Mosteller. 1994. Efficacy of BCG vaccine in the prevention of tuberculosis: meta-analysis of the published literature. *J. Am. Med. Assoc.* 271: 698–702.
6. Kaufmann, S. H. 2006. Tuberculosis: back on the immunologists' agenda. *Immunity* 24: 351–357.
7. Flynn, J. L., and J. Chan. 2001. Immunology of tuberculosis. *Annu. Rev. Immunol.* 19: 93–129.
8. Kaufmann, S. H. 2001. How can immunology contribute to the control of tuberculosis? *Nat. Rev. Immunol.* 1: 20–30.
9. Lalvani, A., R. Brookes, R. J. Wilkinson, A. S. Malin, A. A. Pathan, P. Andersen, H. Dockrell, G. Pasvol, and A. V. Hill. 1998. Human cytolytic and interferon γ-secreting $CD8^+$ T lymphocytes specific for *Mycobacterium tuberculosis*. *Proc. Natl. Acad. Sci. USA* 95: 270–275.
10. Sousa, A. O., R. J. Mazzaccaro, R. G. Russell, F. K. Lee, O. C. Turner, S. Hong, L. Van Kaer, and B. R. Bloom. 2000. Relative contributions of distinct MHC class I-dependent cell populations in protection to tuberculosis infection in mice. *Proc. Natl. Acad. Sci. USA* 97: 4204–4208.
11. Flynn, J. L., M. M. Goldstein, K. J. Triebold, B. Koller, and B. R. Bloom. 1992. Major histocompatibility complex class I-restricted T cells are required for resistance to *Mycobacterium tuberculosis* infection. *Proc. Natl. Acad. Sci. USA* 89: 12013–12017.
12. Orme, I. M. 1987. The kinetics of emergence and loss of mediator T lymphocytes acquired in response to infection with *Mycobacterium tuberculosis*. *J. Immunol.* 138: 293–298.
13. Badovinac, V. P., K. A. Messingham, A. Jabbari, J. S. Haring, and J. T. Harty. 2005. Accelerated $CD8^+$ T-cell memory and prime-boost response after dendritic-cell vaccination. *Nat. Med.* 11: 748–756.
14. Hamilton, S. E., and J. T. Harty. 2002. Quantitation of $CD8^-$ T cell expansion, memory, and protective immunity after immunization with peptide-coated dendritic cells. *J. Immunol.* 169: 4936–4944.
15. Steinman, R. M., and M. Pope. 2002. Exploiting dendritic cells to improve vaccine efficacy. *J. Clin. Invest.* 109: 1519–1526.
16. Nakano, H., T. Nagata, T. Suda, T. Tanaka, T. Aoshi, M. Uchijima, S. Kuwayama, N. Kanamaru, K. Chida, H. Nakamura, et al. 2006. Immunization with dendritic cells retrovirally transduced with mycobacterial antigen 85A gene

elicits the specific cellular immunity including cytotoxic T-lymphocyte activity specific to an epitope on antigen 85A. *Vaccine* 24: 2110–2119.
17. Malowany, J. I., S. McCormick, M. Santosuosso, X. Zhang, N. Aoki, P. Ngai, J. Wang, J. Leitch, J. Bramson, Y. Wan, and Z. Xing. 2005. Development of cell-based tuberculosis vaccines: genetically modified dendritic cell vaccine is a much more potent activator of CD4 and CD8 T cells than peptide- or protein-loaded counterparts. *Mol. Ther.* 13: 766–775.
18. McShane, H., S. Behboudi, N. Goonetilleke, R. Brookes, and A. V. Hill. 2002. Protective immunity against *Mycobacterium tuberculosis* induced by dendritic cells pulsed with both $CD8^+$- and $CD4^+$-T-cell epitopes from antigen 85A. *Infect. Immun.* 70: 1623–1626.
19. Banchereau, J., and A. K. Palucka. 2005. Dendritic cells as therapeutic vaccines against cancer. *Nat. Rev. Immunol.* 5: 296–306.
20. Gulden, P. H., P. Fischer III, N. E. Sherman, W. Wang, V. H. Engelhard, J. Shabanowitz, D. F. Hunt, and E. G. Pamer. 1996. A *Listeria monocytogenes* pentapeptide is presented to cytolytic T lymphocytes by the H2-M3 MHC class Ib molecule. *Immunity* 5: 73–79.
21. Wong, P., and E. G. Pamer. 2003. CD8 T cell responses to infectious pathogens. *Annu. Rev. Immunol.* 21: 29–70.
22. Rodgers, J. R., and R. G. Cook. 2005. MHC class Ib molecules bridge innate and acquired immunity. *Nat. Rev. Immunol.* 5: 459–471.
23. Chun, T., N. V. Serbina, D. Nolt, B. Wang, N. M. Chiu, J. L. Flynn, and C. R. Wang. 2001. Induction of M3-restricted cytotoxic T lymphocyte responses by *N*-formylated peptides derived from *Mycobacterium tuberculosis*. *J. Exp. Med.* 193: 1213–1220.
24. Lauvau, G., and E. G. Pamer. 2001. CD8 T cell detection of bacterial infection: sniffing for formyl peptides derived from *Mycobacterium tuberculosis*. *J. Exp. Med.* 193: F35–F39.
25. Feng, C. G., C. Demangel, A. T. Kamath, M. Macdonald, and W. J. Britton. 2001. Dendritic cells infected with *Mycobacterium bovis* bacillus Calmette Guerin activate $CD8^+$ T cells with specificity for a novel mycobacterial epitope. *Int. Immunol.* 13: 451–458.
26. Harboe, M., S. Nagai, M. E. Patarroyo, M. L. Torres, C. Ramirez, and N. Cruz. 1986. Properties of proteins MPB64, MPB70, and MPB80 of *Mycobacterium bovis* BCG. *Infect. Immun.* 52: 293–302.
27. Roche, P. W., J. A. Triccas, D. T. Avery, T. Fifis, H. Billman-Jacobe, and W. J. Britton. 1994. Differential T cell responses to mycobacteria-secreted proteins distinguish vaccination with bacille Calmette-Guerin from infection with *Mycobacterium tuberculosis*. *J. Infect. Dis.* 170: 1326–1330.
28. Skeiky, Y. A., M. R. Alderson, P. J. Ovendale, J. A. Guderian, L. Brandt, D. C. Dillon, A. Campos-Neto, Y. Lobet, W. Dalemans, I. M. Orme, and S. G. Reed. 2004. Differential immune responses and protective efficacy induced by components of a tuberculosis polyprotein vaccine, Mtb72F, delivered as naked DNA or recombinant protein. *J. Immunol.* 172: 7618–7628.
29. Skeiky, Y. A., M. J. Lodes, J. A. Guderian, R. Mohamath, T. Bement, M. R. Alderson, and S. G. Reed. 1999. Cloning, expression, and immunological evaluation of two putative secreted serine protease antigens of *Mycobacterium tuberculosis*. *Infect. Immun.* 67: 3998–4007.
30. Zhu, X., H. J. Stauss, J. Ivanyi, and H. M. Vordermeier. 1997. Specificity of $CD8^-$ T cells from subunit-vaccinated and infected H-2b mice recognizing the 38 kDa antigen of *Mycobacterium tuberculosis*. *Int. Immunol.* 9: 1669–1676.
31. Dow, S. W., A. Roberts, J. Vyas, J. Rodgers, R. R. Rich, I. Orme, and T. A. Potter. 2000. Immunization with f-Met peptides induces immune reactivity against *Mycobacterium tuberculosis*. *Tuber. Lung Dis.* 80: 5–13.
32. Wang, C. R., A. R. Castano, P. A. Peterson, C. Slaughter, K. F. Lindahl, and J. Deisenhofer. 1995. Nonclassical binding of formylated peptide in crystal structure of the MHC class Ib molecule H2-M3. *Cell* 82: 655–664.
33. Dabhi, V. M., and K. F. Lindahl. 1998. Short peptides sensitize target cells to CTL specific for the MHC class Ib molecule, H2-M3. *Eur. J. Immunol.* 28: 3773–3782.
34. Xu, H., T. Chun, H. J. Choi, B. Wang, and C. R. Wang. 2006. Impaired response to *Listeria* in H2-M3-deficient mice reveals a nonredundant role of MHC class Ib-specific T cells in host defense. *J. Exp. Med.* 203: 449–459.
35. Kerksiek, K. M., D. H. Busch, I. M. Pilip, S. E. Allen, and E. G. Pamer. 1999. H2-M3-restricted T cells in bacterial infection: rapid primary but diminished memory responses. *J. Exp. Med.* 190: 195–204.
36. Seaman, M. S., C. R. Wang, and J. Forman. 2000. MHC class Ib-restricted CTL provide protection against primary and secondary *Listeria monocytogenes* infection. *J. Immunol.* 165: 5192–5201.
37. Levitt, J. M., D. D. Howell, J. R. Rodgers, and R. R. Rich. 2001. Exogenous peptides enter the endoplasmic reticulum of TAP-deficient cells and induce the maturation of nascent MHC class I molecules. *Eur. J. Immunol.* 31: 1181–1190.
38. Chiu, N. M., T. Chun, M. Fay, M. Mandal, and C. R. Wang. 1999. The majority of H2-M3 is retained intracellularly in a peptide-receptive state and traffics to the cell surface in the presence of *N*-formylated peptides. *J. Exp. Med.* 190: 423–434.
39. Sturgill-Koszycki, S., P. H. Schlesinger, P. Chakraborty, P. L. Haddix, H. L. Collins, A. K. Fok, R. D. Allen, S. L. Gluck, J. Heuser, and D. G. Russell. 1994. Lack of acidification in *Mycobacterium* phagosomes produced by exclusion of the vesicular proton-ATPase. *Science* 263: 678–681.
40. Clemens, D. L., and M. A. Horwitz. 1995. Characterization of the *Mycobacterium tuberculosis* phagosome and evidence that phagosomal maturation is inhibited. *J. Exp. Med.* 181: 257–270.

doi: 10.1111/j.1744-313X.2007.00653.x

Association of *IL12RB1* polymorphisms with susceptibility to and severity of tuberculosis in Japanese: a gene-based association analysis of 21 candidate genes

K. Kusuhara,* K. Yamamoto,† K. Okada,‡ Y. Mizuno§ & T. Hara*

Summary

Tuberculosis (TB) is the second commonest cause of death from infectious disease after HIV/AIDS worldwide. Association studies have revealed that host genetic factors, such as human leukocyte antigen and solute carrier family 11 member A1 (NRAMP1), play roles in susceptibility to TB. To identify host genetic factors involved in the susceptibility to TB in Japanese, we performed a gene-based association analysis of 21 candidate genes on 87 TB patients and 265 controls using marker single nucleotide polymorphisms (SNPs). For the genes with two or more marker SNPs exhibiting significant allele association, we subsequently analysed the association between adjacent coding SNPs (cSNPs) and TB. Among a total of 118 marker SNPs, 3 of *IL1B* and 2 of *IL12RB1* showed association with TB. Non-synomymous cSNPs were not identified in *IL1B*. Association studies on four non-synomymous cSNPs of *IL12RB1* (641A/G, 1094T/C, 1132C/G, 1573G/A) in linkage disequilibrium showed that three of them (641A/G, 1094T/C, 1132C/G) were significantly associated with the development of TB. Haplotype analysis on the four cSNPs demonstrated that frequency of ATGG haplotype was significantly lower in TB patients than in controls. When TB patients were divided into two subgroups according to the severity of lung disease, advanced subgroup showed a prominent association with 641A/G, 1094T/C and 1132C/G SNPs. These data suggested that genetic variants of *IL12RB1*, at least in part, confer genetic susceptibility to TB, and are associated with the progression of the disease, in Japanese.

* Department of Pediatrics, Graduate School of Medical Sciences, Kyushu University, Fukuoka, Japan, † Division of Molecular Population Genetics, Department of Molecular Genetics, Medical Institute of Bioregulation, Kyushu University, Fukuoka, Japan, ‡ Division of Pediatrics, Fukuoka National Hospital, Fukuoka, Japan, § Division of Pediatrics, National Fukuoka-Higashi Medical Center, Fukuoka, Japan

Received 26 February 2006; revised 8 June 2006 and 5 October 2006; accepted 26 November 2006

Correspondence: Koichi Kusuhara, MD, PhD, Department of Pediatrics, Graduate School of Medical Sciences, Kyushu University, 3-1-1, Maidashi, Higahi-ku, Fukuoka 812-8582, Japan. Tel: +81-92-6425421; Fax: +81-92-6425435; E-mail: kkusuhar@pediatr.med.kyushu-u.ac.jp

Abbreviations

TB, tuberculosis; IL, interleukin; NRAMP1, natural resistance associated macrophage protein 1; SLC11A1, solute carrier family 11 member A1; VDR, vitamin D receptor; NTM, non-tuberculous environmental mycobacteria; IFN, interferon; MSMD, Mendelian susceptibility to mycobacterial disease; SNP, single, nucleotide polymorphism; cSNP, coding SNPs; IFN-γR, IFN-γ receptor; IL-12R, IL-12, receptor; STAT, signal transducer and activator of transcription; IL-18R, IL-18 receptor; IL-23R, IL-23 receptor; TNF, tumor necrosis factor; TNFRSF, TNF receptor superfamily; UBE3A, ubiquitin protein ligase E3A; LD, linkage disequilibrium; UTR, untranslated region.

Introduction

Tuberculosis (TB) is the second commonest cause of death from infectious disease after HIV/AIDS worldwide. The World Health Organization estimated 8–9 million new cases of clinical TB and 2 million deaths resulting from the disease every year (WHO, 2005). Only about 10% of the individuals infected with *Mycobacterium tuberculosis* develop TB, whereas the remaining 90% stay free from the disease throughout their life (Murray *et al.*, 1990). Almost half of the patients show rapid progression and develop clinical disease within 2 years after infection (Frieden *et al.*, 2003). In addition to these clinical observations, epidemiological, twin and adoption studies support the role of host genetic factors in the susceptibility to TB (Comstock, 1978; Sorensen *et al.*, 1988). Previous association studies demonstrated the association of several genes, such as human leucocyte antigen (HLA), natural resistance associated macrophage protein 1 (NRAMP1 or solute carrier family 11 member A1 [SLC11A1]) and vitamin D receptor (VDR) genes and interleukin (IL)-1 locus, with the susceptibility to TB (Singh *et al.*, 1983; Bellamy *et al.*, 1998, 1999; Goldfeld *et al.*, 1998; Wilkinson *et al.*, 1999; Greenwood *et al.*, 2000). A linkage analysis on sib-pairs conducted in Africa (Bellamy *et al.*, 2000) has mapped TB susceptibility loci to chromosomes 15q11–13 and Xq26, although another genome-wide scan for a Brazilian TB patient did not replicate it (Miller *et al.*, 2004).

On the other hand, genetic analysis of severe or recurrent cases with clinical diseases caused by weakly virulent mycobacterial species, such as BCG and non-tuberculous environmental mycobacteria (NTM) revealed the congenital deficiencies of the molecules involved in IL-12/interferon

